UNIVERSITEIT VAN PRETORIA
UNIVERSITY OF PRETORIA
YUNIBESITHI YA PRETORIA

Selective leaching of phlogopite

by

GS Woest

27540830

A dissertation submitted in partial fulfilment
of the requirements for the degree

Master of Engineering (Chemical Engineering)

Department of Chemical Engineering
Faculty of Engineering, the Built Environment and Information Technology

University of Pretoria
Pretoria

February 2016

UNIVERSITEIT VAN PRETORIA
UNIVERSITY OF PRETORIA
YUNIBESITHI YA PRETORIA

Selective leaching of phlogopite

by

GS Woest

27540830

A dissertation submitted in partial fulfilment
of the requirements for the degree

Master of Engineering (Chemical Engineering)

Department of Chemical Engineering
Faculty of Engineering, the Built Environment and Information Technology

University of Pretoria
Pretoria

February 2016

Selective leaching of phlogopite

Synopsis

The study investigated the acid leaching of phlogopite and the parameters that play a role in the conversion as well as the selectivity of various acids. The parameters investigated were:

- Temperature
- Solid to liquid ratio
- Stir speed
- Acid concentration
- Particle size
- Acid purity

Quantifying the impact each of these parameters have on the conversion and selectivity allows for better understanding and optimization of the leaching of phlogopite. It was found that the ash diffusion rate limited flat plate shrinking core model was the best model at predicting the leaching with the exception of the overall ion leached by hydrochloric acid which was fitted to an empirical equation.

Ash diffusion rate limited flat plate shrinking core model : $X^2 = \frac{t}{\tau}$

Empirical equation : $\frac{dX}{dt} = kC_o(A-X)(1-X)$

KEYWORDS: Phlogopite, Acid leaching, Reaction kinetics

Contents

Nomenclature

A	Liquid solid ratio	l/kg
AC	Acid concentration	%
AP	Acid Purity	g/ml
A_p	Particle area	m^2
b	Stoichiometric constant	(-)
C_b	Bulk concentration	mol/l
C_s	Surface concentration	mol/l
D	Liquid diffusivity	m^2/s
D_e	Effective diffusivity	m^2/s
ΔE	Activation energy	J/mol
d_p	Particle diameter	mm
F_p	Shape factor	(-)
G	Power law integral	(-)
j	Flux	(-)
k	Reaction rate constant	
k_m	Mass transfer coefficient	m/s
L	Half particle thickness	µm
m	Reaction order	(-)
N	Moles	moles
n	Rate of mass transfer	mol/s
PS	Particle size	µm
r	Particle radius	mm
R	Universal gas constant	J/K.mol
R_a	Molar reaction rate	mol/s
Re	Reynold's number	(-)
r_p	Pore radius	mm
Sc	Schmidt's number	(-)
Sh	Sherwood number	(-)
SL	Solid to liquid ratio	g/ml
SS	Stir speed	rpm
S_v	Surface area per unit volume	1/m
t	time	min

T	Temperature	K
u	Particle velocity	m/s
V_p	Particle volume	m^3
X	Conversion	(-)
x	Distance from surface	mm

Greek

ρ	Density	kg/m^3
ρ_m	Molar density	mol/m^3
τ	Time of completion	min
μ	Viscosity	Pa.s

1. Introduction

Over the years Palabora Mining Company (PMC) and Foskor have built up a considerable stockpile of phlogopite in their attempts to mine copper, phosphate and vermiculite. Pockets of phlogopite are scattered across their mining site and have to be removed in order to mine the more valuable minerals. Analysis of the phlogopite from this mine has shown a substantial potassium and magnesium content that could be exploited as a new source of the above mentioned elements.

By means of acid leaching these minerals could possibly be extracted, processed and sold but a greater understanding of the leaching process is required to fully take advantage of this opportunity.

The goal of this study is to investigate the leaching characteristic of various acids on phlogopite and determining the impact each parameter has on the conversion as well as the potassium selectivity of these leaching reactions. Furthermore an attempt was made to find equations to model not only the reaction kinetics but the conversion and selectivity of these reactions as well.

2. Literature

2.1. Structure of phlogopite

According to Harkonen and Keiski (1984) phlogopite is part of the biotite mica group which are made up of parallel silica plates. Figure 1 shows the basic structure of phlogopite to consist of an octahedral sheet containing aluminium (Al), iron (Fe) and magnesium (Mg) sandwiched between two silica tetrahedron layers to form a 2:1 structure.

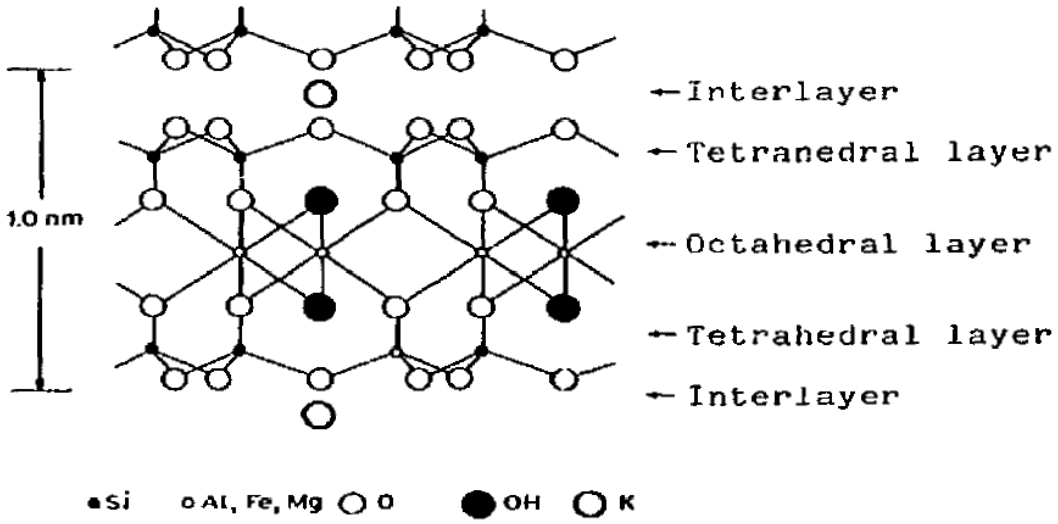

Figure 1: Diagram showing the basic crystalline structure of phlogopite.
(Harkonen and Keiski (1984))

The silicone (Si) in the tetrahedral sheet is partially substituted by Al and Fe. These composite layers are kept together by means of weak bonding with potasium (K) ions. Phlogopite has a pearly to submetallic lustre, a density ranging from 2760 to 2900 kg/m^3 (Khalighi & Minkkinen, 1989) and an overall chemical formula of $K(Mg,Fe)_3Si_3(Al,Fe)O_{10}(OH,F)_2$. The mass composition of phlogopite is given in Table 1.

Table 1: Mass composition of phlogopite (Khalighi & Minkkinen, 1989)

	Weight %
Al_2O_3	10.8
K_2O	10.5
MgO	23.8
FeO,Fe_2O_3	10 as Fe_2O_3
SiO_2	40.5
F	1
H_2O	3.4
Impurities: Ti, Ca, Na, Mn, P	

2.2. Leaching characteristics

The leaching characteristics of phlogopite will predominantly be affected by the dissolution rates of the ions in question. A higher dissolution rate would mean the particular element will be removed preferentially which could be used to our advantage. Kuwahara and Aoki (1995) showed that at the initial stages of leaching the priority of dissolution of metals are in the order of $K^+ > Fe^{3+} > Mg^{2+}$, $Al^{3+} > Si^{4+}$. (It is worth noting that Kuwahara and Aoki used acid containing sodium chloride (NaCl) which could have affected the results as leaching and ion exchange could have occurred simultaneously offsetting the true values). This suggests that the leaching is controlled by the mineral structure. This coincides with observations by Temuujin, Okada and MacKenzie (2003) who found that the ions in the mica interlayer will leach out preferentially with the ions in the tetrahedral layer leaching at a slower rate.

The release of K^+ from the interlayer may also have an effect on the layer charge, potentially decreasing it depending on the phlogopite composition as well as the reagents used (Mamy, 1969). The change in layer charge could have an effect on the leaching characteristics.

The composition of the leaching medium also plays a role as low concentrations of cations such as K^+, Cs^+ and NH_4^+ have been observed causing a blocking effect with regard to K^+ exchange from the interlayer (Mamy, 1969, Scott & Smith, 1966).

However cations such as Na^+ and H^+ in low concentrations increased the diffusion rate of potassium in a calcium – potassium exchange reaction as the smaller ions exchanging with potassium, thereafter undergoing a hydration reaction increasing the interlayer spacing allowing easy access to the calcium (Mamy, 1969).

2.3. Particle structure

It was found that the leachability of tetrahedral ions are lower than octahedral ions by Maqueda, Romero, Morillo and Pérez-Rodríguez (2007) as they found that Al^{3+} and Fe^{3+} were not being completely removed from the tetrahedral sheet of unground vermiculite when lower acid concentrations were used. However Okada, Arimitsu, Kameshima, Nakajima and MacKenzie (2005) found that during the acid leaching of chlorite the Al^{3+} that remained in the samples were present in the octahedral layer suggesting that more leaching took place in the tetrahedral sheet. This could be due to the differences in structure between chlorite and vermiculite. According to Okada, Arimitsu, Kameshima, Nakajima and MacKenzie (2006) the acid leachability of clay minerals is strongly influenced by various factors such as

- Surface area
- The nature of the octahedral cations
- The nature of the tetrahedral cations
- The ratio of expandable layers

Novak and Cicel (1978) observed a decrease in the leaching rate of smectites as the percentage aluminium increased within the octahedral layer. Similarly they found an increase in rate as the aluminium percentage within the tetrahedral layer increased.

Ross and Rich (1973) investigated the relationship between leaching rate and particle thickness of phlogopite and found that an increase in thickness led to a higher substitution of potassium. This relationship is thought to be due to the fact that thicker particles experience more bending and deformation of layers within the phlogopite without the layers splitting as seen in thinner particles, where the bending decreases the selectivity and increases the substitution of K^+.

Barabaszova and Valaskova (2013) investigated the effect of various milling techniques on vermiculite particles and found that vibratory milling causes thinning of the particles and with time, the layered structure is completely destroyed. This method should therefore be avoided if thicker particles are desired as discussed above. Jet or ball mills are preferred when grinding micas for leaching purposes.

2.4. Acid type

Okada et al. (2005) found that the leaching of chlorite with different acids took place at different rates and that sulphuric acid (H_2SO_4) gave the best results followed by nitric acid (HNO_3) and then hydrochloric acid (HCl). This order is not necessarily true for all micas as Harkonen and Keiski (1984) found that HNO_3 gave the best results for phlogopite mined in Finland. This variation in acid effectiveness could be attributed to the mica's structure. Different acids can be considered for the leaching process as shown by Williams and Cloete (2010) where K^+ was selectively leached with citric acid from iron ore while leaving the Fe^{3+} behind.

Okada et al. (2005) found that when Al^{3+} and Fe^{3+} is removed from the tetrahedral sheets it gives passage to the acid, allowing for attack of the deeper layers. In the case of micas with very little Si^{4+} substituted out of their tetrahedral layer the acid can only enter though the particle edges. The effect of gallery versus edge attack (shown in Figure 2) was also observed by Kaviratna and Pinnavaia (1994) which found no intra-gallery ion exchange within phlogopite compared to other micas. This might not be true for all phlogopites as the extent of aluminium substitution within the octahedral layers for the phlogopite used in the analysis could have been preventing leaching as discussed in section 2.3 by Novak and Cicel (1978).

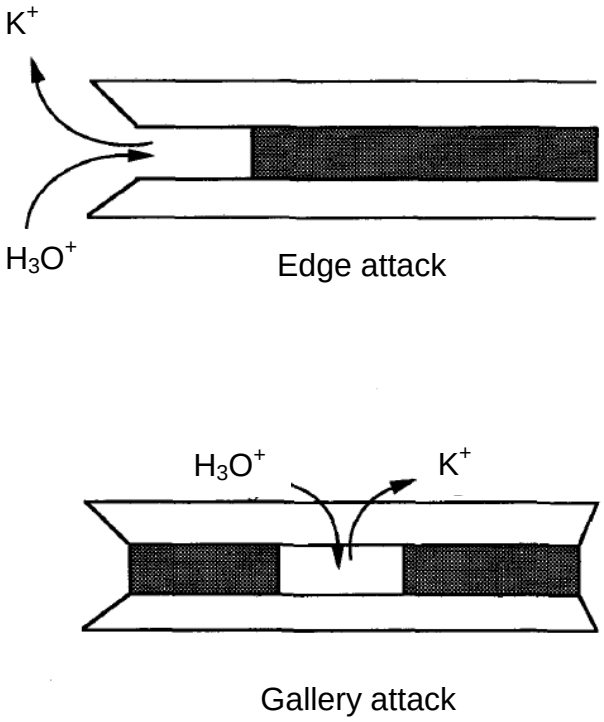

Figure 2: Edge attack mechanism versus gallery attack

2.5. Pore creation

Harkonen and Keiski (1984) showed that acid removes the ions from within the layers causing the layers to separate, open up and create pores in the silica as the sheets entangle. The phlogopite becomes more porous and electrochemically active as hydrogen (H^+) ions are substituted into the interlayers. The increase of H^+ increases the solid acidity of the particle and its adsorption properties (Okada et al, 2006).

The entanglement of layers is increased by grinding the samples before leaching as shown by Maqueda et al (2007) where unground vermiculite kept a certain amount of its layered structure after leaching whereas ground vermiculite's layers were completely destroyed.

Maqueda et al (2007) also found that the grinding process greatly improves the reactivity of the leaching treatment and causes micro pores to form within the particles greatly increasing the surface area of the particles.

Maqueda et al (2007) found that <80 µm vermiculite particles leached at 80℃ at a 1:20 solid to liquid ratio and 1 M HCl produced particles with a surface area of 504.28 m^2/g. However an acid concentration of 0.5 M HCl produced a surface area of only 90.25 m^2/g showing higher concentrations producing higher surface area.

Kaviratna and Pinnavaia (1994) investigated the effect the attack mechanism would have on the surface area of the silica structure and found that it did not play a role. However the expanding nature of the clay has a substantial effect. They found that phlogopite only produced silica structures with a surface area less than 20 m^2/g when leached with 5 M HCl. This is substantially less than the 620 m^2/g reported by Harkonen and Keiski (1984). These differences could be due to a difference in structure or composition between the phlogopites.

The silica structures formed during leaching could be of use as they tend to have very high surface area (504 – 720 m^2/g) as seen in Maqueda et al (2007) which would make them a potentially viable alternative to activated carbon as backbone for catalyst or similar applications. Temuujin et al (2003) found that excessive leaching times tend to destroy the micro pores.

2.6. Acid concentration

It was found that higher acid concentrations (1 M HCl) produced higher surface areas compared to lower concentrations (0.25 – 0.5 M HCl). Temuujin et al (2003) however found that the concentration influence becomes less notable as the concentration increases. At a concentration of 4 M the leaching rate was similar to that of a 2 M concentration which could indicate a maximum with regard to concentration affect. This observation could be due to the reaction rate being controlled by internal mass transfer of the product being formed as the products diffusion rate will not be affected by the acid concentration. Kuwahara and Aoki (1995) also reported secondary Fe^{3+} and Al^{3+} complexes forming at a later stage of leaching which could possibly restrict the diffusion of reagents and products in the particles. These complexes that form were also reported by Maqueda et al (2007) and found to be iron-oxy-hydroxides.

2.7. Leaching kinetics

The elementary steps of a leaching reaction can be summarised as a solid reacting with a fluid to produce a fluid and in some cases a solid product as seen in Equation 1 while taking into account stoichiometric constants.

$$a\text{Fluid} + b\text{Solid} \rightarrow c\text{Leachate} + d\text{Solid} \quad (1)$$

The overall reaction may consist of various determining steps and can be seen in Figure 3. (Sohn & Wadsworth, 1979; 2)

- External mass transfer
- Internal mass transfer
- Chemical reaction

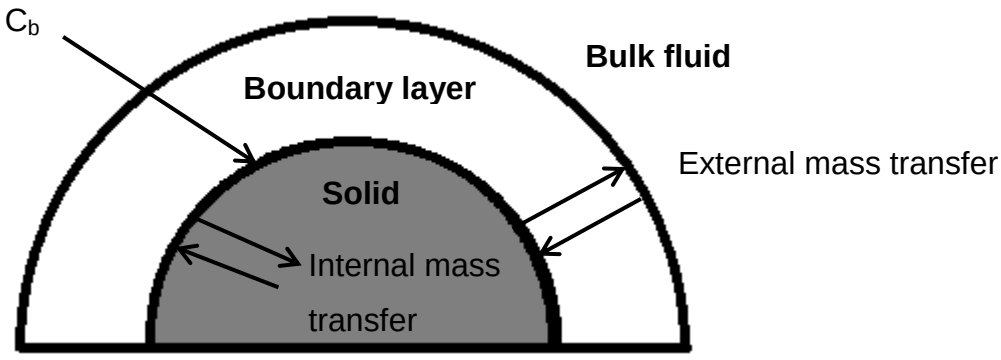

Figure 3: Diffusion over boundary layer of particle

It has been found that the step determining the rate of the overall reaction may change for a reaction depending on the reaction conditions. The step with the lowest rate will determine the overall rate. These steps may also interact, determining the overall rate of the equation. Another process that can have an influence on the leaching rate is the structural change of the solid during the reaction (Sohn & Wadsworth, 1979; 3)

2.7.1 External mass transfer

The external mass transfer is the process whereby reagents diffuse from the bulk fluid to the solid surface and products diffuse from the particle surface to the bulk fluid over the boundary layer. External mass transfer to or from a particle is given in Equation 2.

$$j = k_m(C_b - C_s)A_p \quad (2)$$

The mass transfer coefficient k_m can be calculated by the empirical correlations shown by Equations 3 – 6. (Sohn & Wadsworth, 1979; 4)

$$Sh = 2 + 0.6Re^{1/2}.\ Sc^{1/3} \quad (3)$$

where

$$Sh = k_m\, d_p/D \quad (4)$$

$$Re = d_p\rho u/\mu \quad (5)$$

and

$$Sc = \mu/\rho D \quad (6)$$

Sh, Re and Sc are the dimensionless groups namely Sherwood, Reynolds and Schmidt numbers respectively, d_p is the particle diameter, D is the diffusivity of the liquid, ρ is the liquid density, u is the particle velocity within the liquid and μ is the liquid viscosity. (Sohn & Wadsworth, 1979; 4) It is possible to remove the effect stir speed has on the overall reaction rate by increasing it sufficiently (Sohn & Wadsworth, 1979; 138) as an increase in particle velocity would increase the Reynolds number and therefore increase the mass transfer coefficient. When k_m is large enough to no longer be the limiting factor in the reaction rate stirring speed will no longer play a role.

2.7.2 Internal mass transfer

Internal mass transfer is an important part of the overall reaction when dealing with porous solid reagents as more area is exposed for potential reaction. Internal mass transfer also plays a role when porous solid reagent forms on the particle.
The complexity of mass transfer within the pores is increased by possible variation in pore structure which is not easily predicted. Diffusion within pores is described by Fick's law of diffusion and is shown in Equation 7.

$$j = -D_e . \nabla C \tag{7}$$

where D_e is the effective diffusivity of the species and ∇C is the concentration gradient. (Welty, Wicks, Wilson & Rorrer, 2008; 403) The effective diffusivity takes into account the cross-sectional area taken up by solids as well as inconsistent pore lengths within the particle (Sohn & Wadsworth, 1979; 5).

2.7.3 Chemical reaction

The chemical reaction rate is the rate at which conversion takes place at the surface of the particle and can be expressed by simple differential equations as seen in Equation 8 (Sohn & Wadsworth, 1979; 135).

$$\frac{dN_A}{dt} = R_A = -kC^n \tag{8}$$

where R_A is the molar reaction rate per unit area of solids, k the reaction rate constant, C the concentration of reagent at the point of reaction and n represents the order of the reaction.

Temperature plays a large role in the chemical reaction rate and the influence can be determined by means of the Arrhenius equation (Equation 9). The Arrhenius equation gives the relationship between the reaction rate constant and temperature.

$$k = k_o e^{\frac{-\Delta E}{RT}} \quad (9)$$

where k_o is the theoretical rate constant at an infinite temperature, ΔE is the activation energy, R is the universal gas constant and T is the temperature. It is clear that a higher temperature will always give a higher reaction rate (Fogler, 2004). Ayanda, Adekola, Baba, Fatoki and Ximba (2011) found activation energies of 60.23 kJ/mol, 64.31 kJ/mol and 67.53 kJ/mol for the acid leaching of laterite.

2.8 Leaching models

Various leaching models exist, predicting the overall leaching rate by taking into account the effect of internal and external mass transfer as well as reaction kinetics. Clemency and Lin (1981) developed a linear model for the dissolution of phlogopite in acid solutions with low concentrations. Their conclusion that the kinetics are linear were based on the fact that they only took into account a short time interval of the leaching reaction. When the whole reaction is taken into account, the reaction is found to be highly nonlinear. They reported a constant rate of $2x10^{-14}$ $moles_{phlogopite}/cm^2s$. As phlogopite has a plate structure, the shrinking core models dealing with flat plates were the first to be investigated and compared to other models such as power law models and other empirical leaching models.

2.8.1 Shrinking core

The shrinking core model assumes a non-porous particle with starting radius r_o dissolving over time in a liquid reagent of concentration C_b which is constant. The reaction only takes place at the surface of the particle and will shrink with time. The shrinking core model takes into account three different limiting conditions namely chemical reaction rate, external mass transfer and ash diffusion rate. (Murdoch University(2006))

2.8.1.1 Reaction rate limited

In the case where the chemical reaction rate is limiting (no concentration gradient over boundary layer) $C_s = C_b$ the model for a spherical particle can be written as Equation 10 and 11 (Levenspiel, 1999: 580)

$$X = 1 - (1 - \frac{t}{\tau})^3 \quad (10)$$

$$\tau = \frac{\rho_m r_o}{bC_s k} \quad (11)$$

Where X is the conversion, τ is the time required for the reaction to go to completion, ρ_m is the molar density of the solid particle, r_o is the original particle size. Alternatively the model can be written for flat plate particles and can be seen in Equation 12 and 13 where L is equal to half the particles thickness.

$$X = \frac{t}{\tau} \quad (12)$$

$$\tau = \frac{\rho_m L}{bC_s k} \quad (13)$$

2.8.1.2 External mass transfer

In the case where external mass transfer is the limiting step to the process, the concentration of liquid reagent at the surface $C_s = 0$. The model for external mass transfer controlled for a spherical particle is given in Equation 14 and 15. (Levenspiel, 1999: 580)

$$\frac{t}{\tau} = 1 - (1 - X)^{0.5} \quad (14)$$

$$\tau = \frac{\rho_m r_o}{3bC_s k} \quad (15)$$

The model can also be written for flat plate particles and can be seen in Equation 16 and 17.

$$X = \frac{t}{\tau} \tag{16}$$

$$\tau = \frac{\rho_m L}{bC_s k} \tag{17}$$

It is worth noting that the model is the same as for the reaction rate limited flat plate shrinking core but the k values are not interchangeable as they are not defined by the same basis.

2.8.1.3 Ash diffusion rate limited

In the case where the diffusion rate through the ash layer is limiting a product layer is formed as the reaction takes place on the particle surface. As the reaction moves to completion the reactive core shrinks while the product layer increases. The ash diffusion limited models for spherical as well flat plate particles are shown in Equations 18 to 21. (Levenspiel, 1999:580)

Spherical: $$\frac{t}{\tau} = 1 - 2(1 - x) - 3(1-x)^{2/3} \tag{18}$$

$$\tau = \frac{\rho_m r_o^2}{6bC_b D_e} \tag{19}$$

Flat plate: $$X^2 = \frac{t}{\tau} \tag{20}$$

$$\tau = \frac{\rho_m L^2}{2bC_b D_e} \tag{21}$$

Table 2: Summary of Shrinking core models

	Spherical			Flat Plate		
Conditions	Shrinking core reaction rate limiting	Shrinking core mass transfer limiting	Shrinking core ash diffusion rate limiting	Shrinking core reaction rate limiting	Shrinking core mass transfer limiting	Shrinking core ash diffusion rate limiting
Reaction zone	Particle surface	Particle Surface	Particle surface	Particle surface	Particle Surface	Particle surface
Active concentration	$C_s = C_b$	$C_s = 0$	$C_s = 0$	$C_s = C_b$	$C_s = 0$	$C_s = 0$
Reaction order Particle parameters	1st Spherical, single particle size	1st Spherical, single particle size	1st Spherical, single particle size	1st Flat plate, single particle size	1st Flat plate, single particle size	1st Flat plate, single particle size
Analysis method	Plot $(X - 1)^{1/3}$ vs time τ = gradient $\tau = f(k)$	Plot $(1 - X)^{0.5}$ vs time τ = gradient $\tau = f(k)$	Plot Equation 18 τ = gradient $\tau = f(D_e)$	Plot X vs time τ = gradient $\tau = f(k)$	Plot X vs time τ = gradient $\tau = f(k)$	Plot X^2 vs time τ = gradient $\tau = f(D_e)$

Leaching conditions for all models: Constant temperature, Constant bulk concentration, constant stir rate
Response to be measured for all models: Mineral concentration within leachate

2.8.2 Power law models

Power law models are simple differential equations similar to that shown in Equation 8 and provide a good starting point with regard to fitting models due to their simplicity. Equation 22 to 24 show first, second and third order power law models.

$$\frac{dN_A}{dt} = R_A = -kC \tag{22}$$

$$\frac{dN_A}{dt} = R_A = -kC^2 \tag{23}$$

$$\frac{dN_A}{dt} = R_A = -kC^3 \tag{24}$$

Tabel 3: Summary of power law models

Conditions	First order	Second order	Third order
Analysis method	Plot Ln(C) vs time k = gradient	Plot 1/C vs time k = gradient	Plot $1/2C^2$ vs time k = gradient

Leaching conditions: Constant temperature, Constant bulk concentration, constant stir rate
Response to be measured: Mineral concentration within leachate

2.8.3 Other models

These models consist of empirical equations that could potentially prove useful in describing the leaching process. Some of these equations are empirical variations to theoretical solutions such as Equation 27 which is a pseudo-steady state solution to the ash diffusion limited shrinking core model (Candido & Mathur, 1974).

$$\frac{dX}{dt} = kC_o(A-X)(1-X) \tag{25}$$

$$\frac{dX}{dt} = \frac{kC_o(A-X)(1-X)^{1/3}}{1-(1-X)^{1/3}} \tag{26}$$

$$\frac{dX}{dt} = \frac{kC_o(A - X)(1-X)^{2/3}}{1 - (1-X)^{1/3}} \quad (27)$$

$$kt = (1-X) + X\ln X \quad (28)$$

Where X is the conversion C_o is initial concentration and A is the liquid to solid ratio. These equations will further on be referred to as empirical model 1 to 4.

Table 4: Summary of empirical models

Conditions	Empirical model 1	Empirical model 2	Empirical model 3	Empirical model 4
Analysis method	Integrate Equation 21 and compare to raw data minimizing the sum of squares to find k	Integrate Equation 22 and compare to raw data minimizing the sum of squares to find k	Integrate Equation 23 and compare to raw data minimizing the sum of squares to find k	Plot Equation 24 with k being the slope of the straight line

Leaching conditions: Constant temperature, Constant bulk concentration, constant stir rate
Response to be measured: Mineral concentration within leachate

3. Experimental

3.1. Apparatus

A batch reactor was chosen for the leaching experiments due to the ease at which the parameters chosen could be controlled as well as modelled compared to a plug flow reactor. A 300 ml Erlenmeyer flask (Duran) was placed in a water bath fitted with a temperature controller (Julabo VC) to insure a stable reactor temperature. Stirring was induced by a magnetic stirrer (Lab smart MS-H280-Pro) placed under the water bath. The use of a magnetic stirrer meant the flask could be closed therefore avoiding potential loss of acid due to evaporation as well as avoiding potential contamination.

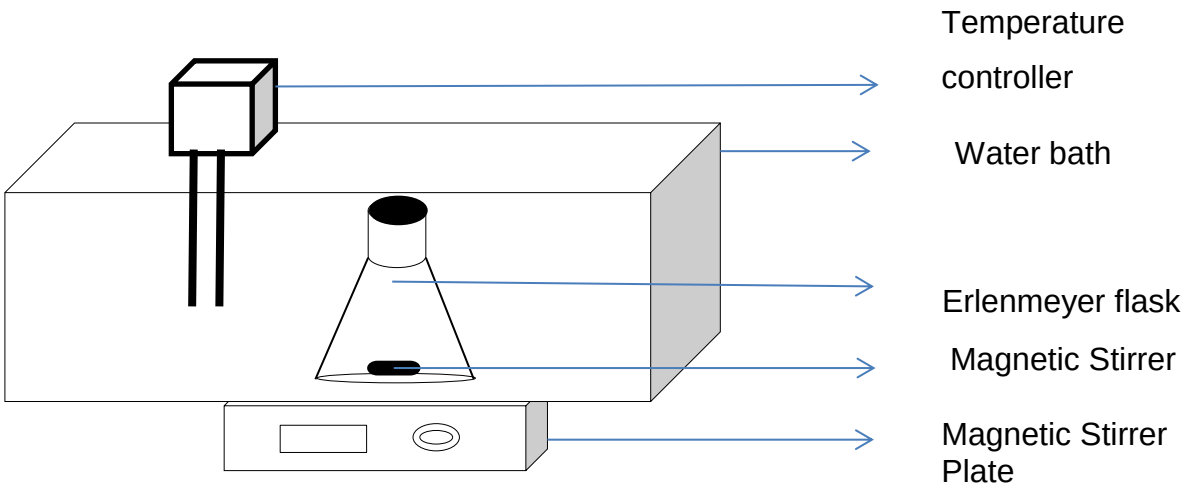

Figure4: Experimental setup diagram

3.2. Planning

From the literature discussed in section 2 the independent variables investigated were as follow:

- Temperature (*T*)
- Particle size (*PS*)
- Acid concentration (*AC*)
- Solid to liquid ratio (*SL*)
- Stir speed (*SS*)
- Acid purity (*AP*)

These parameters were examined by means of a two level partial factorial design in an attempt to minimize the number of initial experiments required to see the effect each parameter has and give an indication to any potential interaction of parameters.

Each experiment was set up by means of a 7x8 orthogonal array shown in Table 5, with 1 and 2 indicating a low or high value of each parameter respectively.

Tabel 5: Orthogonal array

Exp	*T*	*SL*	*SS*	*AC*	*PS*	*AP*
1	1	1	1	1	1	1
2	1	1	1	2	2	2
3	1	2	2	1	1	2
4	1	2	2	2	2	1
5	2	1	2	1	2	1
6	2	1	2	2	1	2
7	2	2	1	1	2	2
8	2	2	1	2	1	1

The average of the responses observed for each level of a parameter is compared as an indication as to the affect the parameter in question has on the chosen response. A difference in the average response seen at the high and low parameter levels indicate that the parameter has an impact on the response, with the

magnitude of the difference giving an indication as to the extent of the impact, whether it is positive or negative.

The upper and lower values of each parameter were chosen with various considerations in mind such as the laboratory temperature exceeding the parameter temperature, sieve sizes available, sampling ease etc. The values are shown in Table 6a.

Table 6a: Upper and lower parameter values

Parameter	Lower level	Upper level
Temperature	30℃	50℃
Solid:liquid	0.1 g/ml	0.2 g/ml
Stir speed	300 rpm	500 rpm
Acid concentration	Half	Full
Particle size	< 75 µm	150 - 250 µm
Acid purity	none	1 g/100ml solution

The three acids found to give the best results by Okada et al. (2005) will be investigated along with citric and acetic acid to investigate the affect weak acids have on the leaching process. The acid concentration in Table 6a is reported as half or full as different acids had different concentration ranges. The full concentrations are given in Table 6b.

Table 6b: Full concentration of various acids

Acid	Full concentration	pH
Hydrochloric acid	32 %	-1.03
Nitric Acid	55 %	-1.07
Sulphuric acid	50 %	-1.19
Citric acid	63 %	1.46
Acetic acid	100 %	2.4

3.3. Sample Preparation

Phlogopite from Palabora complex was crushed using a blender (Kenwood True Compact Blender BL370) and separated by means of a shaker tray and a set configuration of sieves. Particle size analyses of the separated particles were performed to find the size distribution as well as the d_{50} of each sieved range. X-ray fluorescence (XRF) analysis of the phlogopite was done to find the chemical composition.

3.4. Method

3.4.1 Experimental method

3.4.1.1 Experimental setup

The experiments were conducted according to the partial factorial design specified in section 3.2.

The desired temperature of each experiment was set on a temperature controller fitted to the water bath to ensure constant temperature throughout the experiment.

The volume of acid (concentration as specified) required to ensure the correct solid to liquid ratio was measured and transferred to an Erlenmeyer flask and placed in the water bath to reach the desired temperature.

20 g of the desired particle size was weighed on a digital scale (Precisa 1620 C) and added to the acid. The mixture was covered and stirred by means of a magnetic stirrer set to the appropriate speed

3.4.1.2 Sampling

Sampling was performed by turning the stirring off for a minute to allow the fine particles to settle allowing a clear liquid sample to be taken by means of a micro pipet (Thermo Finnpipette 100 - 1000µl). A 1 ml sample was taken and diluted by 99 ml of distilled water and analysed for the different elements leached by means of ICP. The dilution was required to ensure that the sample's concentration was within

the limits of the ICP as well as limiting the affect sampling has on the solid to liquid ratio. Samples were taken at 30, 60, 90, 120, 180, 240, and 360 minutes respectively.

Experiments were repeated after the initial analysis was done to ensure accuracy. Repeats were chosen at random and done in various order to eliminate any unknown bias.

3.4.2 Analytical method

3.4.2.1 Particle size analysis

The particle size analysis of the sieved samples was performed by means of a Malvern mastersizer 3000. A wet analysis was performed on the samples with the matersizer's stir speed set to 2000 rpm and no ultrasound was used as no agglomeration of particles was observed.

3.4.2.2 X-ray fluorescence

XRF was performed on the phlogopite samples to ensure the exact quantities of each element present in the samples. Analysis was performed using a Thermo Fisher ARL9400 XP+ Sequential XRF with WinXRF software. The samples were ground with a tungsten-carbide milling pot to a particle size less than 75 µm, dried at 100℃ and roasted at 1000℃. A 1 g Sample was mixed with 6 g Lithiumteraborate flux and fused at 1050℃ to make a stable fused glass bead. For trace element analyses the sample was mixed with a polyvinyl alcohol (PVA) binder and pressed into a pellet using a 10 ton press.

4. Results and discussion

4.1 Sample analysis

4.1.1 X-ray Fluorescence

The XRF analysis of the phlogopite used in this study is shown in Table 7.

Table 7: XRF analysis of phlogopite

Compound	SiO_2	TiO_2	Al_2O_3	Fe_2O_3	MgO	CaO	K_2O	LOI
%	42.63	1.03	10.42	7.22	25.36	0.76	6.98	6.57

The analysis shows that the phlogopite consists mainly of Si, Al, Fe, Mg^{2+} and K^{+}. These mass percentages indicate the element in its oxide form, the true mass percentage of each major element is shown in Table 8.

Table 8: Elemental mass percentages of phlogopite

Element	%
Si^{4+}	19.89
Al^{3+}	5.52
Fe^{3+}	5.05
Mg^{2+}	15.21
K^{+}	5.79

4.1.2 Particle Size Analysis

The PSA results for the ground phlogopite samples used in this study are shown in Figures 5.

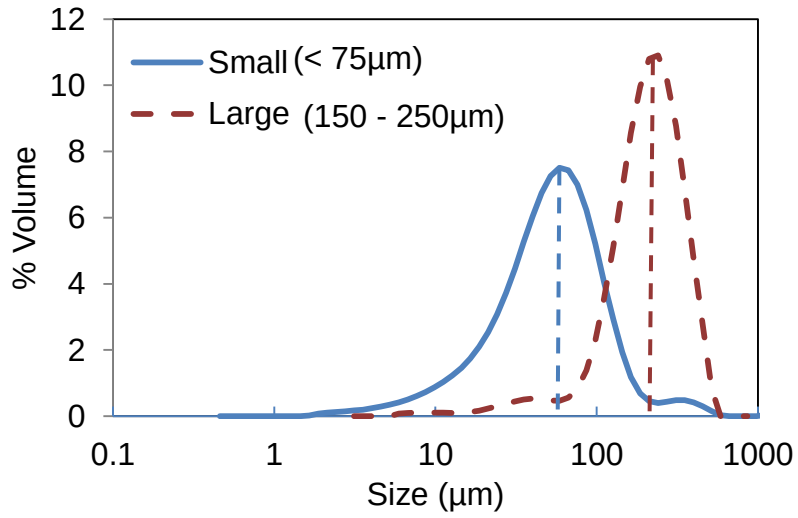

Figure 5: Particle size analysis of ground phlogopite (small)

The d_{v50} of the samples were found to be 57.3 and 226 µm respectively.

4.2 Leaching results

The concentrations of K^+, Mg^{2+}, Al and Fe in solution were measured throughout the leaching experiments for the different acids and can be seen in Appendix A. The three results investigated were as follow.

- Potassium conversion
- The overall conversion of all leachable elements
- Potassium selectivity

The Potassium and overall conversions (X) were calculated by dividing the concentration of the element in solution by the maximum concentration theoretically obtainable from the mass of phlogopite used as shown in Equation 29 and 30.

$$X_K = \frac{C_{K\ solution}}{C_{K\ max}} \times 100 \quad (29)$$

$$X_{Overall} = \frac{\sum C_{solution}}{\sum C_{max}} \times 100 \quad (30)$$

The potassium selectivity is expressed as a percentage of K^+ in the overall ions solution at a given time as shown in Equation 31. The selectivity values used in this section for analysis are all calculated after 6 hours.

$$\text{Selectivity} = \frac{n_K}{\sum n_{ions}} \times 100 \quad (31)$$

4.2.1 Hydrochloric acid

The above mentioned results we calculated for each experiment with hydrochloric acid and shown in Table 9 with the best result highlighted for each.

Tabel 9: Conversions and selectivity for hydrochloric acid

Exp	*T*	*SL*	*SS*	*AC*	*PS*	*AP*	X_K	$X_{Overall}$	K^+ Selectivity %
1	1	1	1	1	1	1	0.379	0.400	20.13
2	1	1	1	2	2	2	0.160	0.131	25.59
3	1	2	2	1	1	2	0.189	0.208	20.05
4	1	2	2	2	2	1	0.255	0.291	18.96
5	2	1	2	1	2	1	0.746	0.778	20.95
6	2	1	2	2	1	2	0.452	0.559	17.62
7	2	2	1	1	2	2	0.529	0.552	20.95
8	2	2	1	2	1	1	0.557	0.629	19.05

Table 9 shows that the parameters in experiment 5 gave the best conversion not only for potassium but for the overall ion content of the phlogopite whereas experiment 2 delivered the best selectivity.

Figures 6 and 7 show the potassium and overall conversions for selected experiments.

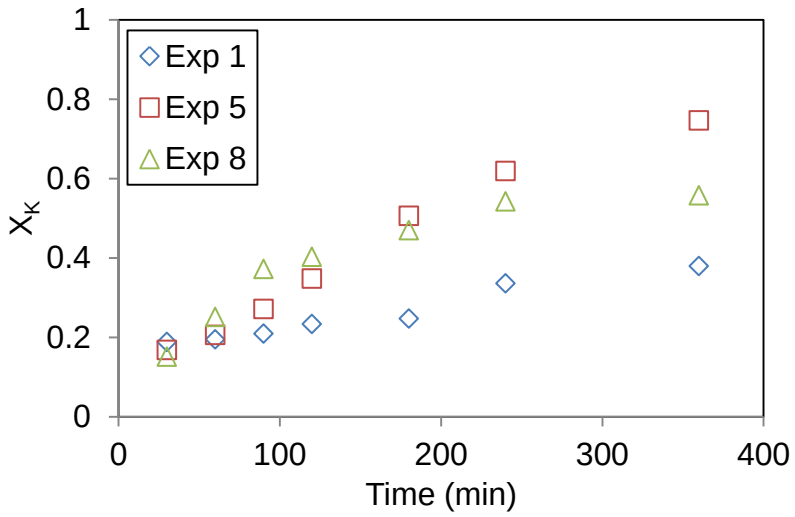

Figure 6: Potassium conversion over time for various experiments

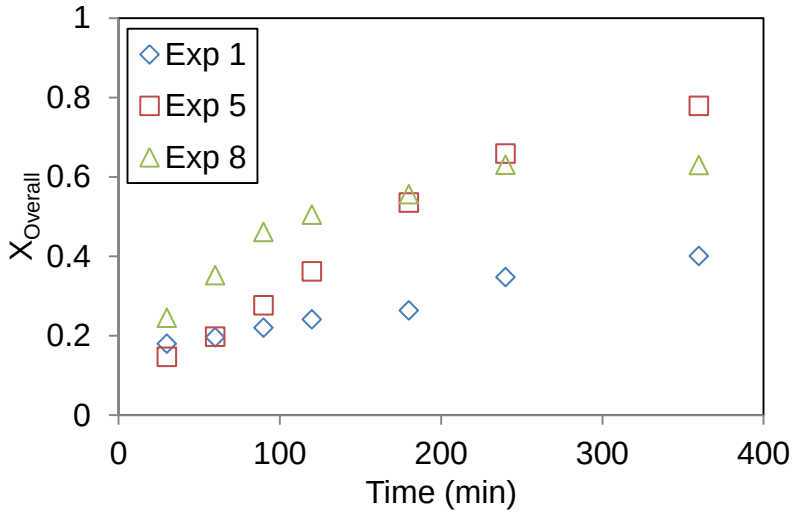

Figure 7: Overall conversion over time for various experiments

4.2.1.1 Potassium Conversion

The main effects contributing towards the potassium conversion was calculated and is shown in Figure 8. The combination of parameters that Figure 8 predicts would lead to the highest conversion coincides with experiment 5 shown in Table 9 which did produce the best result.

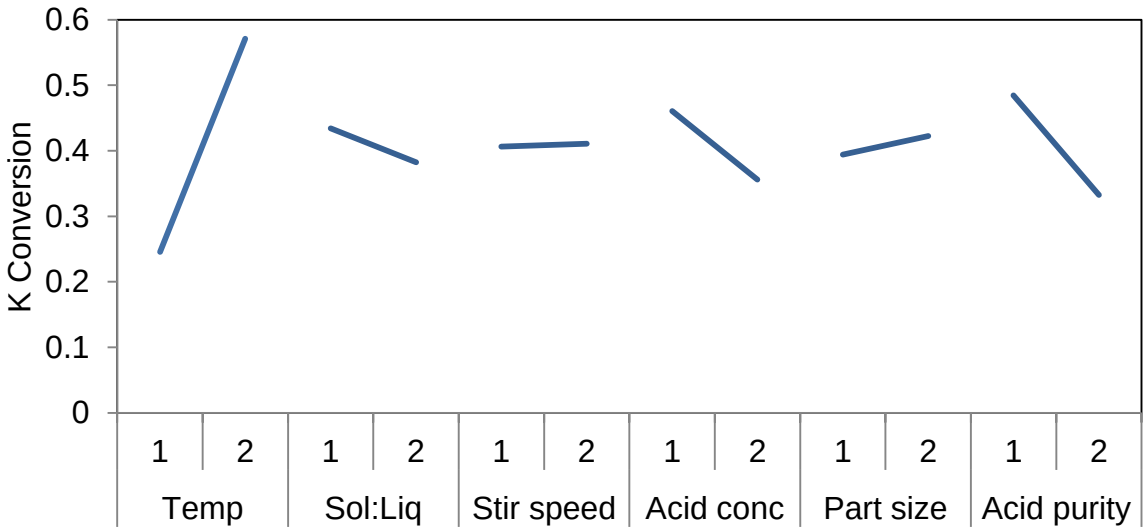

Figure 8: Main effects of potassium conversion with HCl

From Figure 8 it can be seen that the two factors that play the biggest role in conversion is temperature and acid purity with acid concentration playing a small role as confirmed by the ANOVA analysis in Table 10 showing the percent contribution (P) of each parameter.

Table10: ANOVA analysis of potassium conversion achieved with HCl

Parameter	Variance	F	P
T	0.212	1248	73.85
SL	0.006	31.64	1.87
SS	$4x10^{-5}$	0.216	0.01
AC	0.022	129.1	7.63
PS	0.002	9.232	0.55
AP	0.046	270.9	16.03
Error	$2x10^{-4}$	1	0.06

A linear equation modelling the conversion as a function of the parameters can be derived from this analysis and they are shown in Equation 32.

$$X_K = 16.27x10^{-3}T - 6.538x10^{-3}AC - 0.0303AP - 4.916 \quad (32)$$

The contribution of temperature is positive as expected as the Arrhenius equation shows that hotter conditions will always lead to faster reactions. The negative effect of *AP* could indicate inhibiting action as discussed in section 2.2 or potentially reabsorption of ions into the structure.

4.2.1.2 Overall conversion

The main effects contributing towards the overall conversion was calculated and is shown in Figure 9. The combination of parameters that Figure 9 predicts would lead to the highest conversion coincides with experiment 5 shown in Table 9 which did produce the best result.

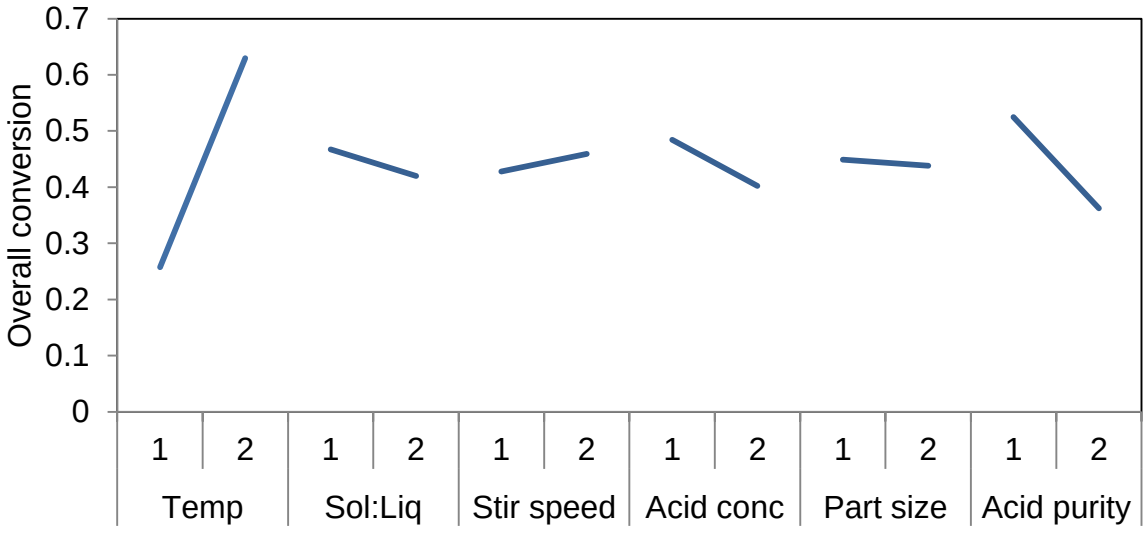

Figure 9: Main effects of overall conversion with HCl

From Figure 9 it can be seen that the two factors that play the biggest role in conversion is temperature and acid purity as confirmed by the ANOVA analysis in Table 11 showing the percent contribution of each parameter.

Table11: ANOVA analysis of overall conversion achieved with HCl

Parameter	Variance	F	P
T	0.277	706.0	79.15
SL	0.004	11.27	1.26
SS	0.002	4.903	0.55
AC	0.013	34.31	3.85
PS	$2x10^{-4}$	0.617	0.07
AP	0.053	133.9	15.01
Error	$4x10^{-4}$	1	0.11

A linear equation modelling the conversion as a function of the parameters can be derived from this analysis and they are shown in Equation 33.

$$X_{Overall} = 18.59x10^{-3}T - 0.0323AP - 5.458 \quad (33)$$

The contribution of temperature is positive as expected, as the Arrhenius equation shows that hotter conditions will always lead to faster reactions. The negative effect the *AP* has, could indicate reaction inhibition or potentially reabsorption of ions into the solids.

4.2.1.3 Potassium selectivity

The main effects contributing towards the potassium selectivity was calculated and is shown in Figure 10. The combination of parameters that Figure 10 predicts would lead to the highest selectivity coincides with the conditions in experiment 2 which did produce the best result with the exception of acid concentration.

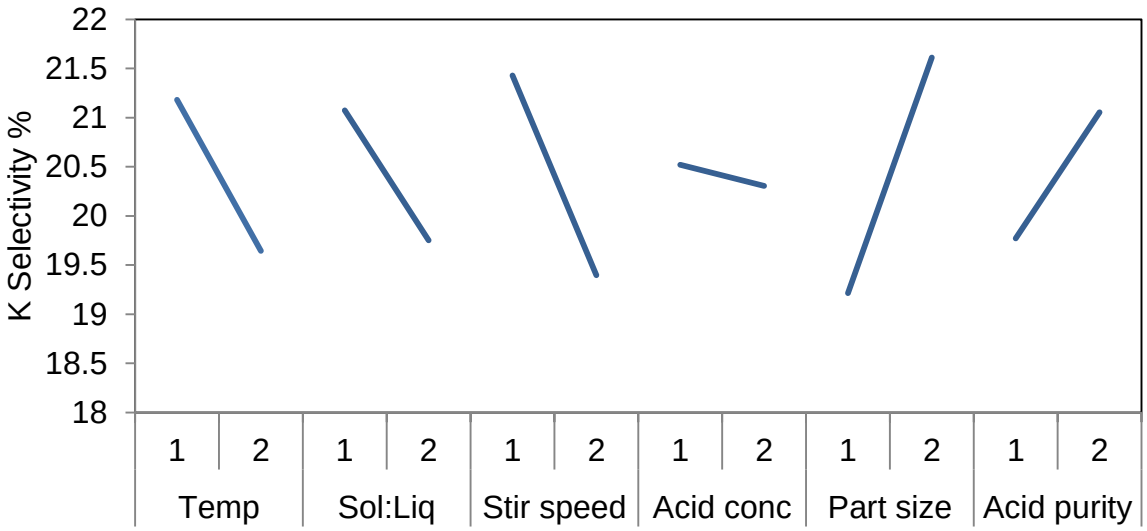

Figure 10: Main effects of potassium selectivity with HCl

Figure 10 shows that every parameter except acid concentration plays a major role in the selectivity of K^+ during leaching with HCl. The ANOVA analysis shown in Table 12 however shows that the percentage contributions of each of these parameters are relatively low.

Table12: ANOVA analysis of potassium selectivity achieved with HCl

Parameter	Variance	F	P
T	4.743	0.596	12.05
SL	3.485	0.438	8.85
SS	8.283	1.041	21.04
AC	0.092	0.012	0.23
PS	11.52	1.447	29.27
AP	3.277	0.412	8.33
Error	7.960	1	20.22

A linear equation modelling the conversion as a function of the parameters can be derived from this analysis and they are shown in Equation 34.

$$K^+ \text{ Selectivity} = -77.09\text{x}10^{-3}T - 13.2SL - 10.18\text{x}10^{-3}SS + 13.66\text{x}10^{-3}PS + 6.4AP + 55.69 \quad (34)$$

The negative effect temperature has on the selectivity could be due to the potassium leaching reaction having a lower activation energy than the other reactions. The positive effect particle size plays on the selectivity could be an indication that the other ions not present in the interlayer are affected more by internal mass transfer than the potassium in the interlayers. The effect acid purity plays could be due to ions suffering more from the inhibiting effect discussed in section 2.2 or due to reabsorption of ions into the structure.

4.2.2 Nitric acid

The results we calculated for each experiment with nitric acid and shown in Table 13 with the best result highlighted for each.

Tabel 13: Conversions and selectivity for nitric acid

Exp	*T*	*SL*	*SS*	*AC*	*PS*	*AP*	X_K	$X_{Overall}$	K^+ Selectivity %
1	1	1	1	1	1	1	0.581	0.349	35.16
2	1	1	1	2	2	2	0.386	0.161	47.78
3	1	2	2	1	1	2	0.621	0.279	46.90
4	1	2	2	2	2	1	0.429	0.194	45.78
5	2	1	2	1	2	1	0.984	0.849	25.28
6	2	1	2	2	1	2	0.839	0.721	25.43
7	2	2	1	1	2	2	1.00	0.828	28.25
8	2	2	1	2	1	1	0.708	0.671	28.13

Table 12 shows that the parameters in experiment 7 gave the best conversion for potassium whereas experiment 5 gave the best overall conversion and again experiment 2 delivered the best selectivity.

The potassium as well as the overall conversions of various experiments are shown in figure 11 and 12.

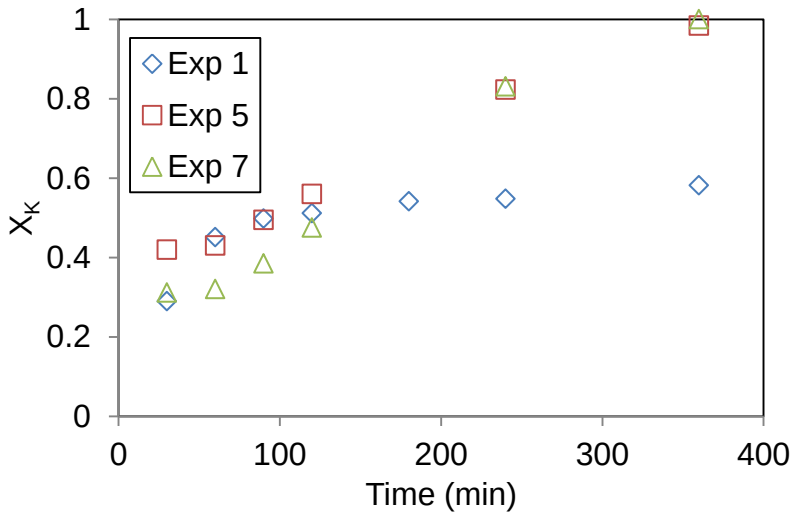

Figure 11: Potassium conversion over time for various experiments

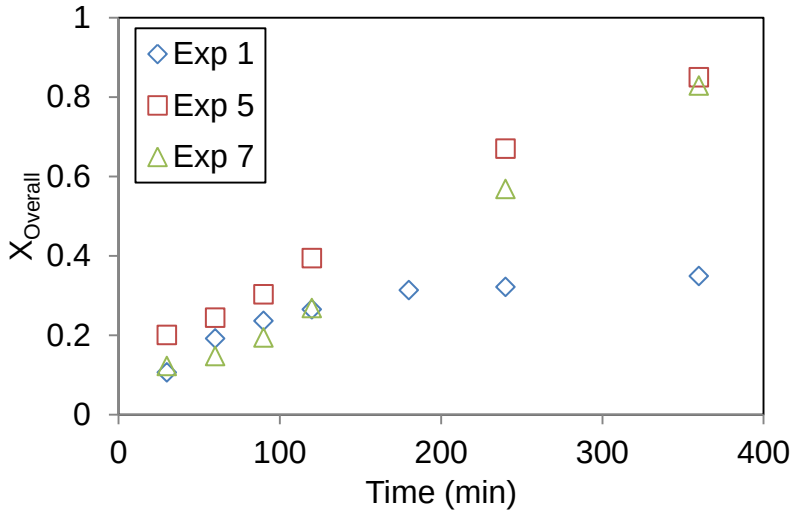

Figure 12: Overall conversion over time for various experiments

4.2.1.1 Potassium Conversion

The main effects contributing towards the potassium conversion was calculated and is shown in Figure 13. The combination of significant parameters that Figure 13 predicts would lead to the highest conversion coincides with experiment 5 and 7 shown in Table 13 which did produce the best result.

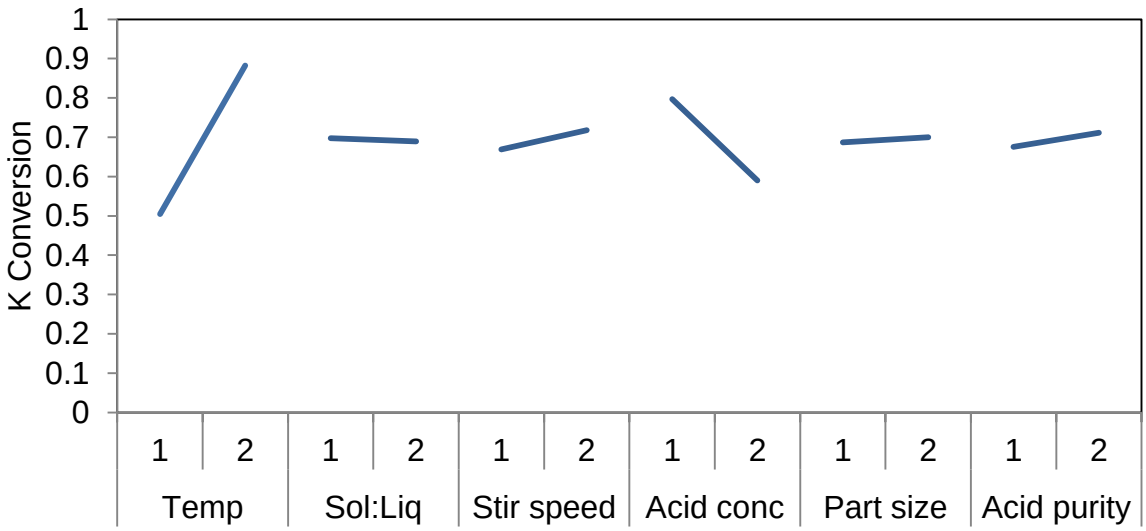

Figure 13: Main effects of potassium conversion with nitric acid

From Figure 13 it can be seen that the two factors that play the biggest role in conversion is temperature and acid concentration as confirmed by the ANOVA analysis in Table 14 showing the percent contribution (P) of each parameter.

Table14: ANOVA analysis of potassium conversion achieved with nitric acid

Parameter	Variance	F	P
T	0.287	101.9	74.98
SL	$1x10^{-4}$	0.046	0.03
SS	0.005	1.742	1.28
AC	0.085	30.18	22.21
PS	$3x10^{-4}$	0.111	0.08
AP	0.003	0.922	0.68
Error	0.003	1	0.74

A linear equation modelling the conversion as a function of the parameters can be derived from this analysis and they are shown in Equation 35.

$$X_K = 19.86x10^{-3}T - 8.184x10^{-3}AC - 5.852 \quad (35)$$

The contribution of temperature is positive as expected as the Arrhenius equation shows that hotter conditions will always lead to faster reactions. The negative effect the acid concentration has could indicate the presence of an optimum acid concentration similar to what was discussed in section 2.6.

4.2.1.2 Overall conversion

The main effects contributing towards the potassium conversion was calculated and is shown in Figure 14. The combination of significant parameters that Figure 14 predicts would lead to the highest conversion coincides with experiment 5 and 7 shown in Table 13 which did produce the best result.

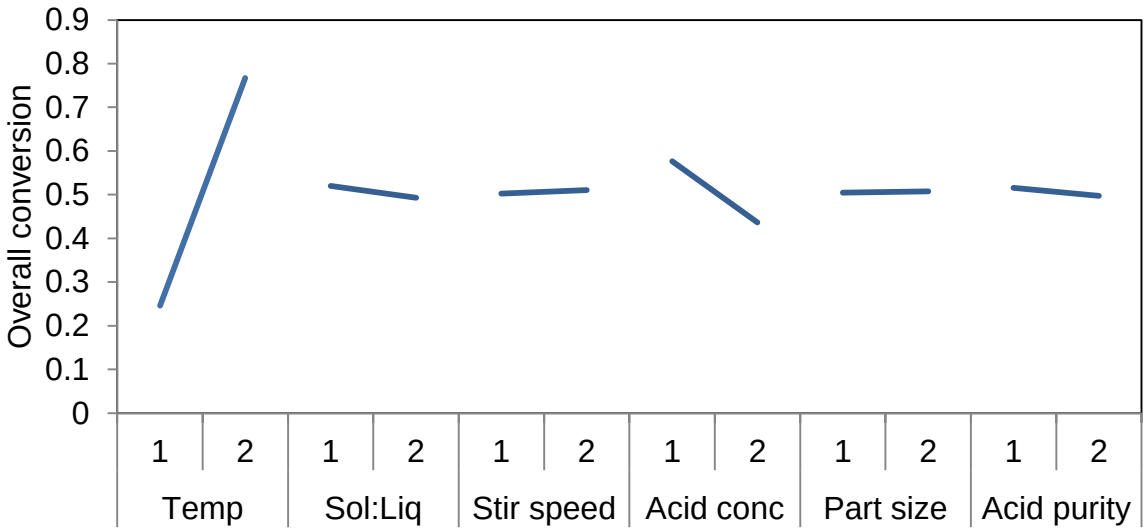

Figure 14: Main effects of overall conversion with nitric acid

From Figure 14 it can be seen that the two factors that play the biggest role in conversion is temperature and acid concentration as confirmed by the ANOVA analysis in Table 15 showing the percent contribution (P) of each parameter.

Table15: ANOVA analysis of overall conversion achieved with nitric acid

Parameter	Variance	F	P
T	0.544	249.7	92.61
SL	0.002	0.669	0.25
SS	$1x10^{-4}$	0.066	0.02
AC	0.039	17.87	6.63
PS	$2x10^{-5}$	0.008	0.00
AP	$7x10^{-4}$	0.314	0.12
Error	0.002	1	0.37

A linear equation modelling the conversion as a function of the parameters can be derived from this analysis and is shown in Equation 36.

$$X_{Overall} = 26.07x10^{-3}T - 5.069x10^{-3}AC - 7.862 \quad (36)$$

The contribution of temperature is positive as expected as the Arrhenius equation shows that hotter conditions will always lead to faster reactions. The negative effect the acid concentration has could be an indication of an optimum acid concentration.

4.2.1.3 Potassium selectivity

The main effects contributing towards the potassium selectivity was calculated and is shown in Figure 15. The combination of parameters that Figure 15 predicts would lead to the highest selectivity not coinciding with experiment 2,which as shown in Table 13, produced the best result. This could be due to the lack of statistical significance of some of the parameters.

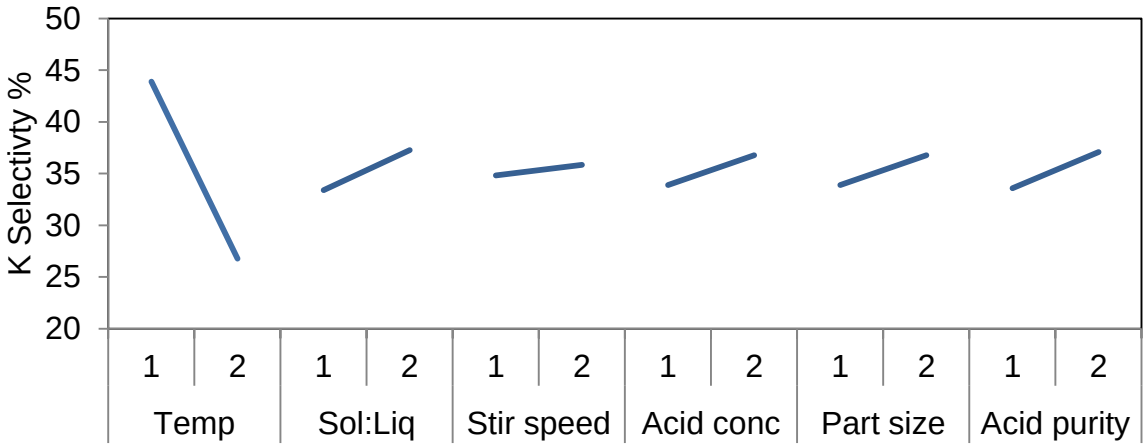

Figure 15: Main effects of potassium selectivity with nitric acid

Figure 15 shows that only temperature plays a major role in the selectivity of K^+ during leaching with nitric acid as confirmed by the ANOVA analysis shown in Table 16

Table 16: ANOVA analysis of potassium selectivity achieved with nitric acid

Parameter	Variance	F	P
T	587.05	25.884	83.97
SL	29.684	1.3088	4.25
SS	2.0706	0.0913	0.30
AC	16.618	0.7327	2.38
PS	16.445	0.7251	2.35
AP	24.535	1.0818	3.51
Error	22.68	1	3.24

A linear equation modelling the conversion as a function of the parameters can be derived from this analysis and they are shown in Equation 37.

$$K^+ \text{ Selectivity} = -0.8566T \quad (37)$$

The negative effect temperature has on the selectivity could be due to the potassium leaching reaction having a lower activation energy than the other reactions.

4.2.3 Sulphuric acid

Exploratory experiments were conducted to establish whether sulphuric acid would be a suitable leaching medium when compared to other acids. It was found that sulphuric acid was not as effective as hydrochloric or nitric in the leaching of phlogopite as the best conversion achieved in 6 hours was 34 % compared to 74.6 and 98.4 % of hydrochloric and nitric acid respectively at the same conditions. Therefore the decision was made to not investigate sulphuric acid further due to the lack of effectiveness.

4.2.4 Citric acid

Exploratory experiments were conducted to establish whether citric acid would be a suitable leaching medium when compared to other acids. It was found that citric acid was not as effective as hydrochloric or nitric in the leaching of phlogopite as the best conversion achieved in 6 hours was 14.5 % compared to 25.5 and 43.0 % of hydrochloric and nitric acid respectively at the same conditions. Therefore the decision was made to not investigate citric acid further due to the lack of effectiveness.

4.2.5 Acetic acid

Exploratory experiments were conducted to establish whether acetic acid would be a suitable leaching medium when compared to other acids. The use of acetic acid was found to be unsuccessful in the leaching of phlogopite as no substantial elements were extracted during these experiments and will not be discussed further in this study.

4.2.6 Leaching summary

The results shown in section 4.2 are summarised in Table 17 for a quick overview and direct comparison between the various acids.

Table 17: Leaching results summary

Acid	Hydrochloric	Nitric
Average K^+ conversion %	0.4083	0.6935
Average overall conversion %	0.4440	0.5068
Average K^+ selectivity %	20.41	35.33
Significant parameters for conversion	*T*, *AC* and *AP*	*T* and *AC*
Significant parameters for selectivity	*T, SL, SS, PS* and *AP*	*T* (other parameters play a substantially smaller role)

Table 17 clearly shows that nitric acid performed the best with regard to conversion as well as potassium selectivity followed by hydrochloric. Citric, sulphuric and acetic acid did not show significant leaching and will not be discussed further in this study.

4.3 Model fitting

4.3.1 Fitting

The various models discussed in section 2 were fitted to the experimental data for the various acids and can be seen in Appendix B. The models fitted are summarized in Table 19. The methods used to fit these models vary and will be briefly discussed.

The power law models were integrated to find linear relations shown in Equation 38 with the G term defined for each model in Table 18.

$$G = kt \tag{38}$$

Table 18: G definition for each power law model

Model	G
First order	$\ln C$
Second order	$\frac{1}{C}$
Third order	$\frac{1}{2C^2}$

These G values were calculated for each data point and plotted versus time. If the model were to fit the resulting plot, it would give a straight line with the slope being equal to the reaction constant k.

The Shrinking core models as well as empirical model 4 can be fitted with a similar linearization method, with the whole of the right hand side of the equation being lumped together. This leaves one with a linear equation, with the time being the subject of the equation and τ being the slope. The lumped group were calculated for each data point and plotted versus time. If the model fits the data the resulting plot should be a straight line.

Empirical models 1 to 3 were numerically integrated by means of the Euler method using the first data point as the starting point. The sum of the error squared between the predicted and measured value for each data point was minimized to find the best possible fit and the corresponding k value.

Table 19: Summary of models fitted to leaching data.

	Model	Equation	Constant
Shrinking Core	Ash diffusion rate limited (flat plate)	$X^2 = \frac{t}{\tau}$	$\tau = \frac{\rho_m L^2}{2bC_bD_e}$ (min)
	Reaction rate limited (spherical)	$\frac{t}{\tau} = 1 - (1 - X)^{1/3}$	$\tau = \frac{\rho_m r_o}{bC_sk}$ (min)
	External mass transfer limited (spherical)	$\frac{t}{\tau} = 1 - (1 - X)^{0.5}$	$\tau = \frac{\rho_m r_o}{3bC_sk}$ (min)
	Ash diffusion rate limited (spherical)	$\frac{t}{\tau} = 1 - 2(1 - x) - 3(1-x)^{2/3}$	$\tau = \frac{\rho_m r_o^2}{6bC_bD_e}$ (min)
Power Law	First order	$\frac{dN_A}{dt} = R_A = -kC$	k (min^{-1})
	Second order	$\frac{dN_A}{dt} = R_A = -kC^2$	k ($M^{-1}min^{-1}$)
	Third order	$\frac{dN_A}{dt} = R_A = -kC^3$	k ($M^{-2}min^{-1}$)
Empirical	Model 1	$\frac{dX}{dt} = kC_o(A-X)(1-X)$	k ($M^{-1}min^{-1}$)
	Model 2	$\frac{dX}{dt} = \frac{kC_o(A-X)(1-X)^{1/3}}{1-(1-X)^{1/3}}$	k ($M^{-1}min^{-1}$)
	Model 3	$\frac{dX}{dt} = \frac{kC_o(A-X)(1-X)^{2/3}}{1-(1-X)^{1/3}}$	k ($M^{-1}min^{-1}$)
	Model 4	$kt = (1-X) + X\ln X$	k (min^{-1})

4.3.1.1 Hydrochloric acid

All the models in Table 19 were fitted to the experimental data for hydrochloric acid and the resulting fits compared. The R^2 values for the models are shown in Appendix C with the best fit highlighted for each experiment.

Appendix C shows that the potassium leaching with hydrochloric acid was best modelled by the four shrinking core models with the flat plate ash diffusion rate limited model being selected due to its overall good performance as well as its simplicity. The overall leaching of ions was very well modelled at low temperatures by the spherical external mass transfer limited shrinking core model but when all the experiments are considered empirical model 1 gave the best consistent fit to the data. Table 20 shows the R^2 values for the two selected models respectively.

Table 20: R^2 values for the best model fits using hydrochloric acid

Exp	*T*	*SL*	*SS*	*AC*	*PS*	*AP*	R^2_K	$R^2_{Overall}$
1	1	1	1	1	1	1	0.944	0.969
2	1	1	1	2	2	2	0.586	0.943
3	1	2	2	1	1	2	0.812	0.948
4	1	2	2	2	2	1	0.966	0.967
5	2	1	2	1	2	1	0.974	0.979
6	2	1	2	2	1	2	0.753	0.829
7	2	2	1	1	2	2	0.962	0.968
8	2	2	1	2	1	1	0.846	0.803

The main effects playing a role on the R^2 values of the models would indicate whether there are certain parameter ranges where these models do not perform well, therefore the robustness of each model are shown in Figures 16 and 17 for potassium and overall leaching respectively.

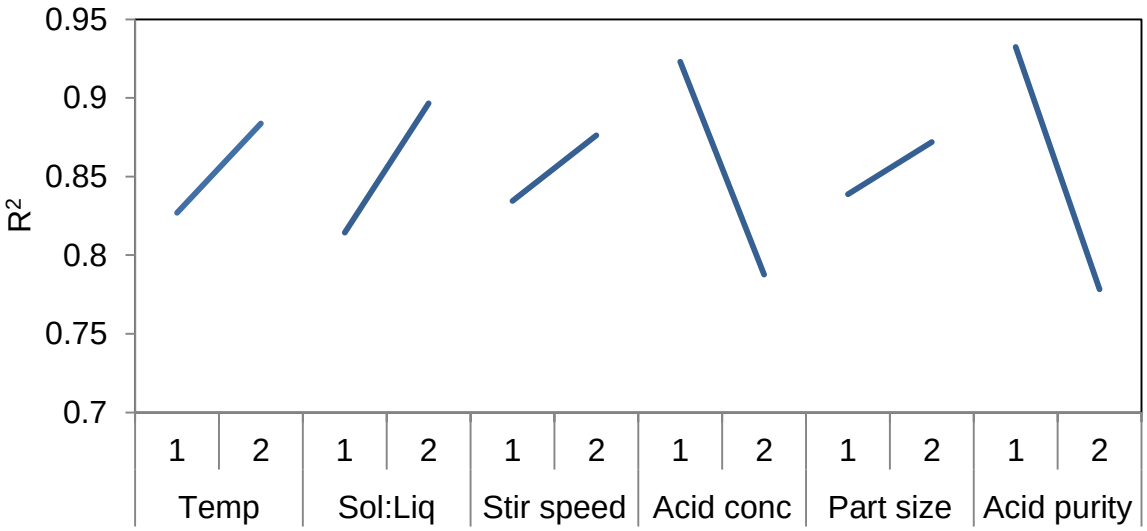

Figure 16: Main effects of the R^2 value for the flat plate ash diffusion limited shrinking core model predicting K^+ leaching

Figure 17: Main effects of the R^2 value for empirical model 1 for predicting overall ions leached

The effects seen in Figures 16 and 17 look to play a large role but the Anova analysis in Table 21 shows that the impact these parameters have are only slight but should be taken into account when using these models to avoid potential errors.

Table 21: Anova analysis of the R^2 for best fitting models

	Potassium leaching			Overall leaching		
Parameter	Variance	F	P	Variance	F	P
T	0.0064	0.311	4.93	0.0077	17.084	23.01
SL	0.0135	0.653	10.36	0.0001	0.321	0.43
SS	0.0035	0.168	2.67	0.0002	0.444	0.60
AC	0.0366	1.767	28.02	0.0130	28.801	38.79
PS	0.0022	0.107	1.69	0.0119	26.351	35.49
AP	0.0476	2.299	36.45	0.0001	0.250	0.34
Error	0.0207	1	15.86	0.0005	1	1.35

4.3.1.2 Nitric acid

All the models in Table 19 were fitted to the experimental potassium data for nitric acid and the resulting fits compared. The R^2 values for the models are shown in Appendix C with the best fit highlighted for each experiment.

Appendix C shows that the potassium as well as the overall leaching with nitric acid was best modelled by the four shrinking core models with the flat plate ash diffusion rate limited model being selected due to its overall good performance as well as its simplicity. Table 22 shows the R^2 values for these fits with the flat plate ash diffusion rate limited model.

Table 22: R^2 values for the best model fits using nitric acid

Exp	*T*	*SL*	*SS*	*AC*	*PS*	*AP*	R^2_K	$R^2_{Overall}$
1	1	1	1	1	1	1	0.819	0.9388
2	1	1	1	2	2	2	0.784	0.9850
3	1	2	2	1	1	2	0.701	0.9306
4	1	2	2	2	2	1	0.949	0.9916
5	2	1	2	1	2	1	0.966	0.9722
6	2	1	2	2	1	2	0.963	0.9860
7	2	2	1	1	2	2	0.984	0.9790
8	2	2	1	2	1	1	0.958	0.9923

The main effects playing a role on the R^2 values of the models would indicate whether there are certain ranges where these models do not predict the required values, therefore the robustness of each model are shown in Figures 18 and 19 for potassium and overall leaching respectively.

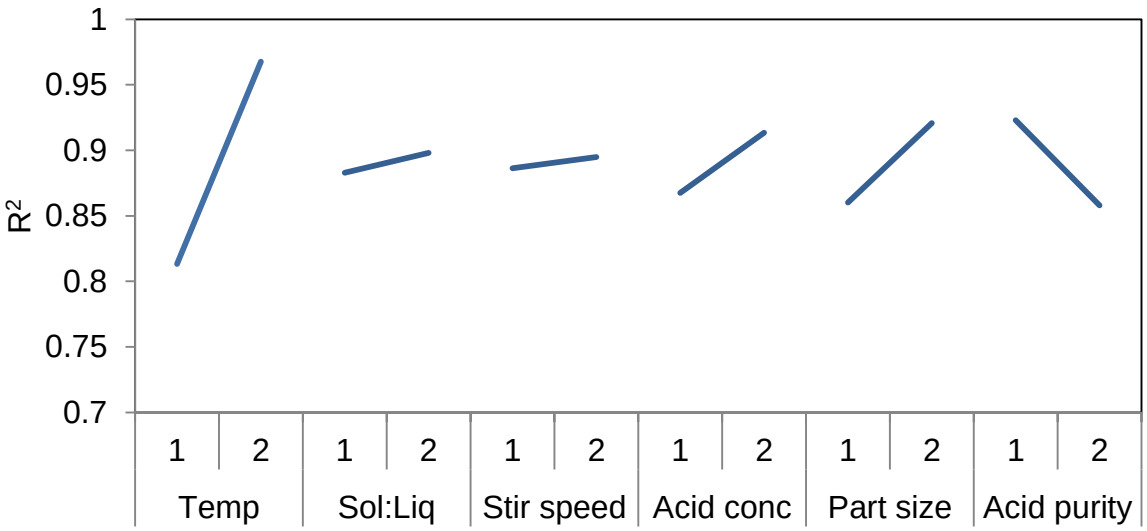

Figure 18: Main effects of the R^2 value for the flat plate ash diffusion limited shrinking core model predicting K^+ leaching

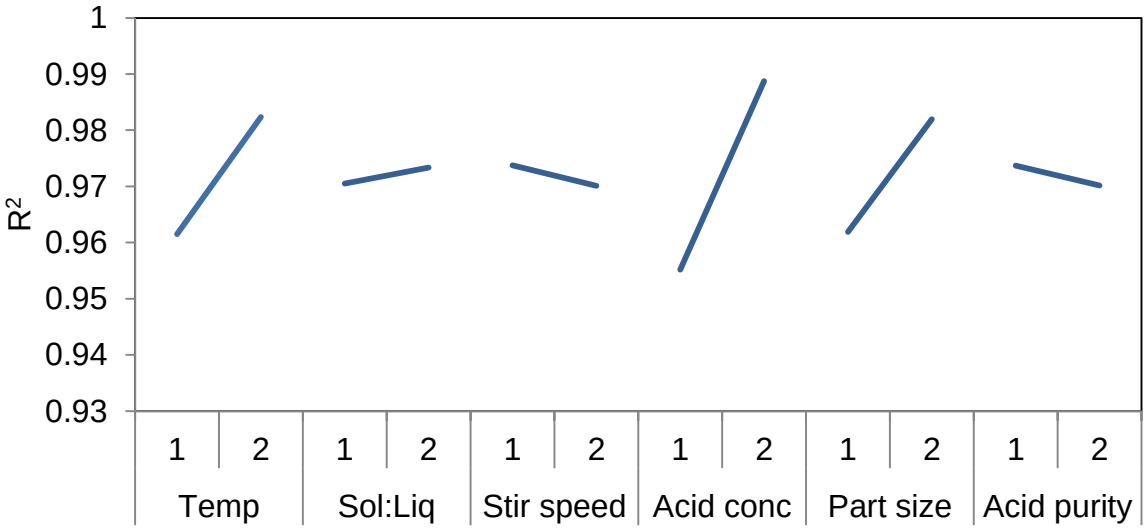

Figure 19: Main effects of the R^2 value for empirical model 1 for predicting overall ions leached

The effects seen in Figures 18 and 19 look to play a large role but the Anova analysis in Table 23 shows that only temperature has a significant impact on the accuracy of the model when predicting potassium leaching. Temperature, acid concentration and particle size influences the modelling of the overall leaching reaction. This should be taken into account when using these models to avoid potential errors.

Table 23: Anova analysis of the R^2 for best fitting models

	Potassium leaching			Overall leaching		
Parameter	Variance	F	P	Variance	F	P
T	0.048	4.079	59.64	$9x10^{-4}$	29.785	21.65
SL	$4x10^{-4}$	0.038	0.56	$1.7x10^{-5}$	0.565	0.41
SS	$1x10^{-4}$	0.012	0.18	$2.7x10^{-5}$	0.923	0.67
AC	0.004	0.362	5.29	0.002	77.049	55.99
PS	0.007	0.625	9.15	$8x10^{-4}$	27.408	19.92
AP	0.009	0.722	10.56	$2.6x10^{-5}$	0.874	0.64
Error	0.012	1	14.62	$2.9x10^{-5}$	1	0.73

4.2.2 Model analysis

4.2.2.1 Potassium leaching with hydrochloric acid

Section 4.2.1 showed that the four shrinking core models tested gave the best results with the average R^2 value between them varying by less than 0.01. It was therefore decided to choose the simplest model that successfully predicts the experimental data, namely the flat plate ash diffusion rate limited shrinking core model. The X^2 vs time graphs were analysed for each experiment and the slope calculated to find the τ values as seen in Figure 20. The main effects that play a role on the models τ value are shown in Figure 21 and an ANOVA analysis is shown in Table 24.

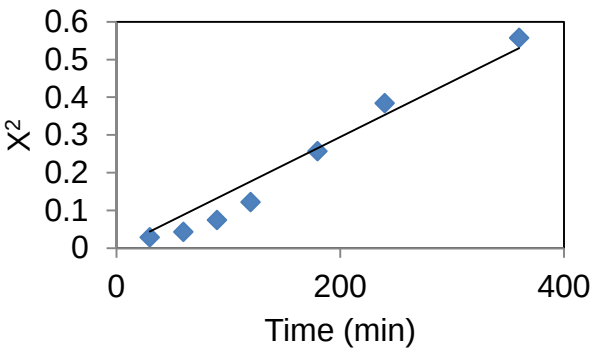

Figure 20: Ash diffusion rate controlled shrinking core fitting to experiment 5

Table 24: ANOVA analysis of τ for potassium leaching with HCl

Parameter	Variance	F	P
T	$6x10^7$	5.7929	61.40
SL	175676	0.0169	0.18
SS	757070	0.0726	0.77
AC	$9x10^6$	0.825	8.75
PS	$6 x10^6$	0.6203	6.57
AP	$1 x10^7$	1.1065	11.73
Error	$1 x10^7$	1	10.60

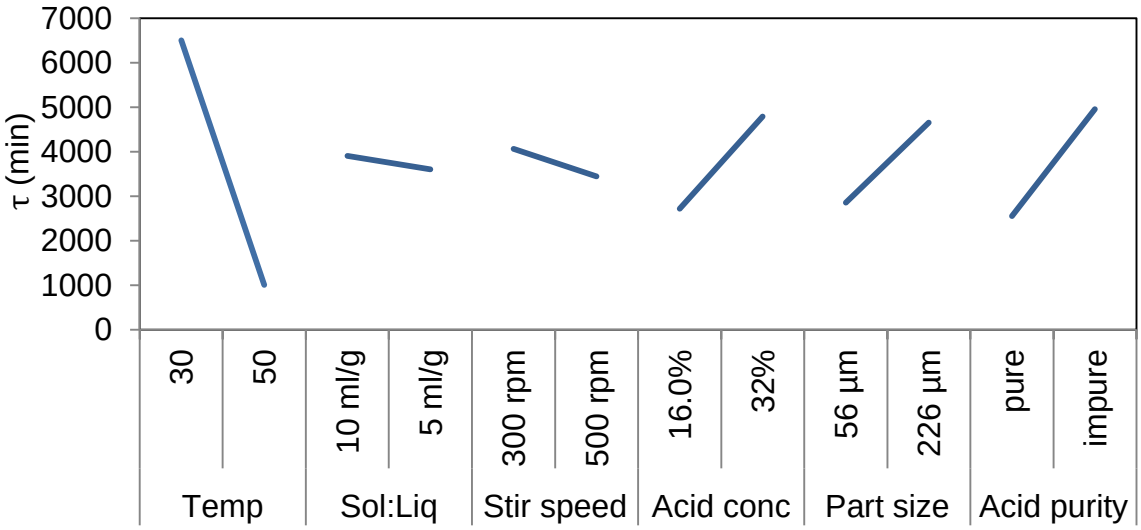

Figure 21: Main effects of τ for the leaching of potassium with HCl

This analysis shows that τ is a function of temperature with acid concentration, particle size and acid purity playing a small role. When compared to Equation 21 the effect temperature has can be attributed to the relation $D_e \propto T$. The impact particle size has on τ can be explained by an increase in plate thickness. The response observed by changing the acid purity may be due to a change in the products concentration gradient or possibly the formation of complexes inhibiting leaching. The effect of acid concentration is however inverse to what is shown in Equation 21. This may be attributed to the fact that the phlogopite does not form a true ash layer or due to it losing its layered structure as well as the presence of two attack mechanisms in gallery and edge attack. The leaching reaction merely emulates the model but is not a true example of ash diffusion limited. Therefore a pseudo equation for τ can be formulated from the analysis above. This pseudo equation is given in Equation 39 and is only assumed valid within the parameter ranges examined.

$$\tau = -274.8T - 129.6AC + 10.22PS + 12008AP + 100308 \quad (39)$$

This equation is a useful representation but is restricted by the fact that τ cannot be negative therefore the true equation is nonlinear as τ becomes smaller.

4.2.2.2 Overall ion leaching with hydrochloric acid

The overall leaching with hydrochloric acid was fitted with empirical model 1 and can be seen in Figure 22. Using Equation 25 a rate constant k can be calculated for each experiment and is shown in Table 25. Figure 23 and Table 26 show the main effects and an ANOVA of the k value.

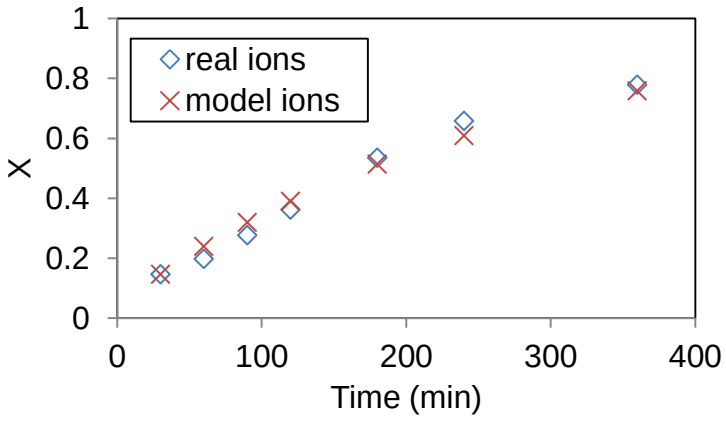

Figure 22: Model predictions versus measured values

Table 25: Calculated rate constants for each experiment

Experiment	Rate constant ($min^{-1}X^{-1}$)
1	$2.44x10^{-4}$
2	$6.80x10^{-5}$
3	$1.10x10^{-4}$
4	$2.06x10^{-4}$
5	$9.37x10^{-4}$
6	$7.79x10^{-4}$
7	$4.99x10^{-4}$
8	$6.96x10^{-4}$

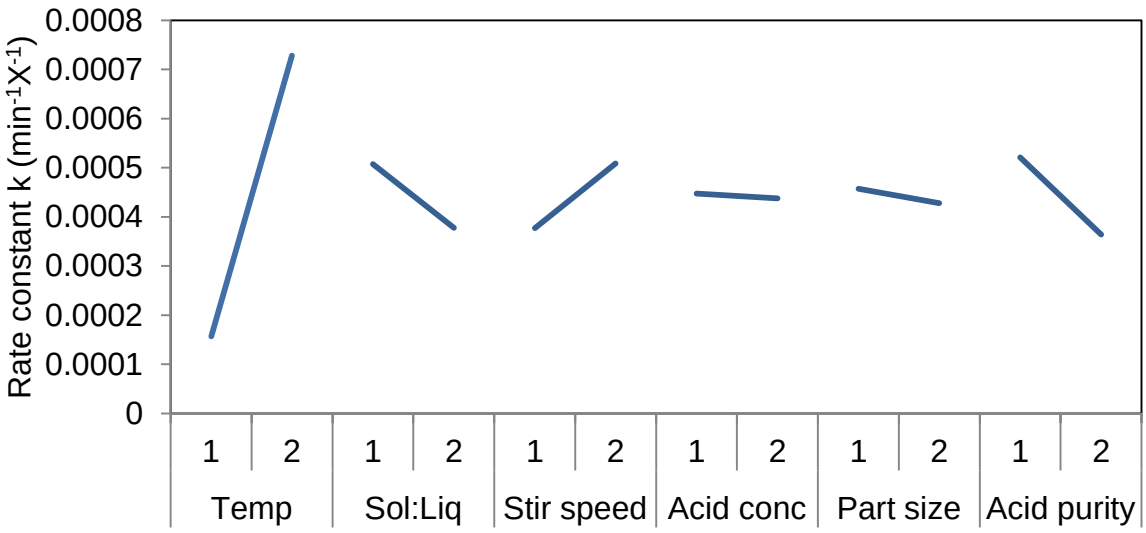

Figure 23: Factorial analysis of rate constant for empirical model 1

Table 26: ANOVA analysis of the rate constant for empirical model 1

Parameter	Variance	F	P
T	$7x10^{-7}$	755.57	84.42
SL	$3x10^{-8}$	38.81	4.34
SS	$3x10^{-8}$	40.17	4.49
AC	$2x10^{-10}$	0.235	0.03
PS	$2x10^{-9}$	2.048	0.23
AP	$5x10^{-8}$	57.14	6.38
Error	$9x10^{-10}$	1	0.11

Table 26 shows that the major contributor to the rate constant is temperature with acid purity, stir speed and solid to liquid ratio playing a very small role. The temperature contribution can be described by the Arrhenius equation and is shown in Figure 24.

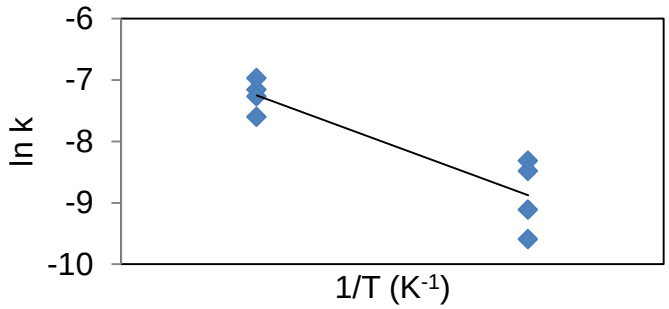

Figure 24: Arrhenuis plot showing the relation between ln k and 1/T for empirical model 1

From the graph the values of k_o and the activation energy ΔE can be determined and was found to be $889x10^4$ $min^{-1}X^{-1}$ and 62.4 kJ/mol respectively. This activation energy seems reasonable when compared to other activation energies for acid leaching as discussed in section 2.7.3.

The overall ion leaching with hydrochloric acid can be given by Equation 40 and 41. The A value which gave the best fit was determined by trial and error and found to be 4.

$$\frac{dX}{dt} = k(4-X)(1-X) \tag{40}$$

$$k = 889x10^4 e^{\frac{-62400}{RT}} \tag{41}$$

4.2.2.3 Potassium leaching with Nitric acid

Section 4.2.1 showed that the four shrinking core models tested gave the best results with the average R^2 value between them varying by less than 0.01. It was therefore decided to choose the simplest model that successfully predicts the

experimental data, namely the flat plate ash diffusion rate limited shrinking core model. The X^2 vs time graphs were analysed for each experiment and the slope calculated to find the τ values as seen in Figure 25. The main effects that play a role on the models τ value are shown in Figure 26 and an ANOVA analysis is shown in Table 27.

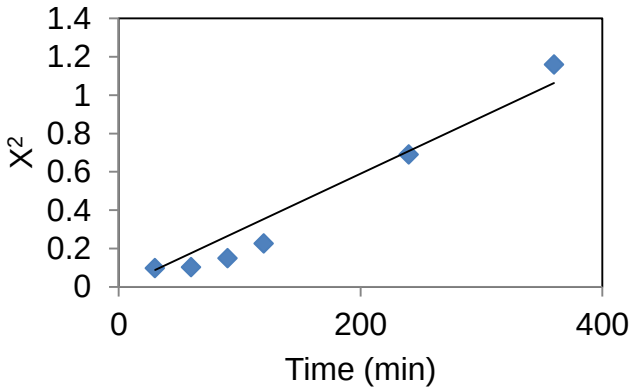

Figure 25: Ash diffusion rate controlled shrinking core fitting to experiment 7

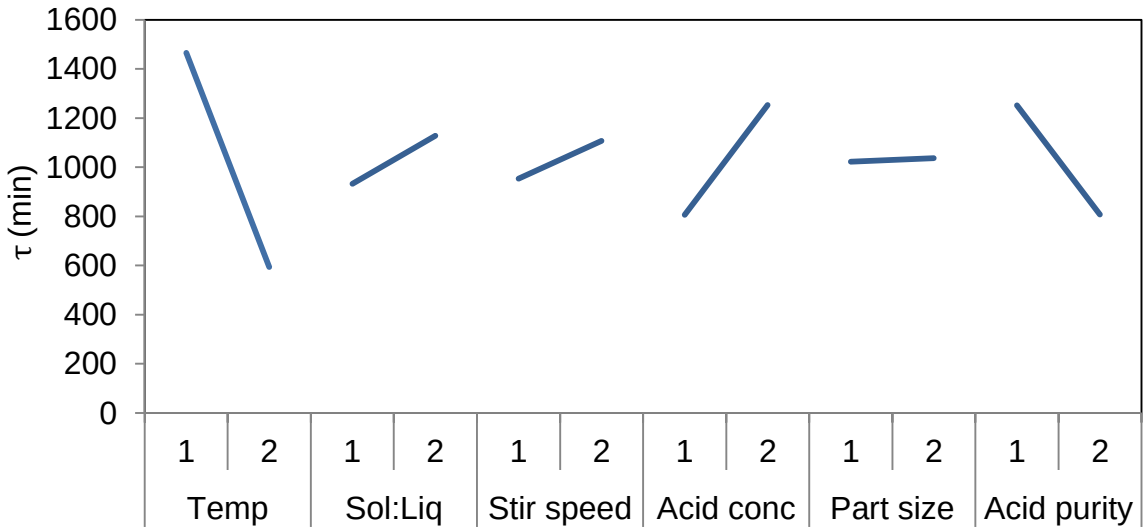

Figure 26: Main effects of τ for the leaching of potassium with Nitric acid

Table 27: ANOVA analysis of τ for potassium leaching with nitric acid

Parameter	Variance	F	P
T	$2x10^6$	10.75	58.89
SL	76501	0.543	2.97
SS	47280	0.335	1.84
AC	400137	2.837	15.54
PS	460.68	0.003	0.02
AP	393122	2.788	15.27
Error	141022	1	5.48

Comparing the results to Equation 21 the effect that temperature has can be explained by the D_e value being a function of temperature. However the τ value does not appear to be a function of particle size as in Equation 21. The effect acid concentration has is inverse to what is expected. Therefore, an empirical equation describing τ as a function of temperature, acid concentration and acid impurities can be derived from the analysis above allowing for the calculation of a pseudo τ value. The empirical equation is given in Equation 42.

$$\tau = -43.53T + 16.26AC - 88.67AP + 15106 \quad (42)$$

This equation is limited by the fact that τ cannot be negative. Therefore nonlinear behaviour is expected as τ becomes smaller.

4.2.2.3 Overall leaching with Nitric acid

Section 4.2.1 showed that the two ash diffusion rate limited shrinking core models tested gave the best results with the average R^2 value between then varying by less than 0.01. It was therefore decided to choose the simplest model that successfully predicts the experimental data, namely the flat plate ash diffusion rate limited shrinking core model. The X^2 vs time graphs were analysed for each experiment and the slope calculated to find the τ values as seen if Figure 27. The main effects that play a role on the models τ value are shown in Figure 28 and an ANOVA analysis is shown in Table 28.

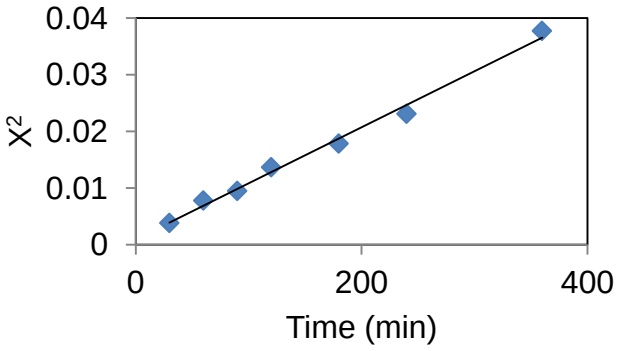

Figure 27: Ash diffusion rate controlled shrinking core fitting to experiment 4

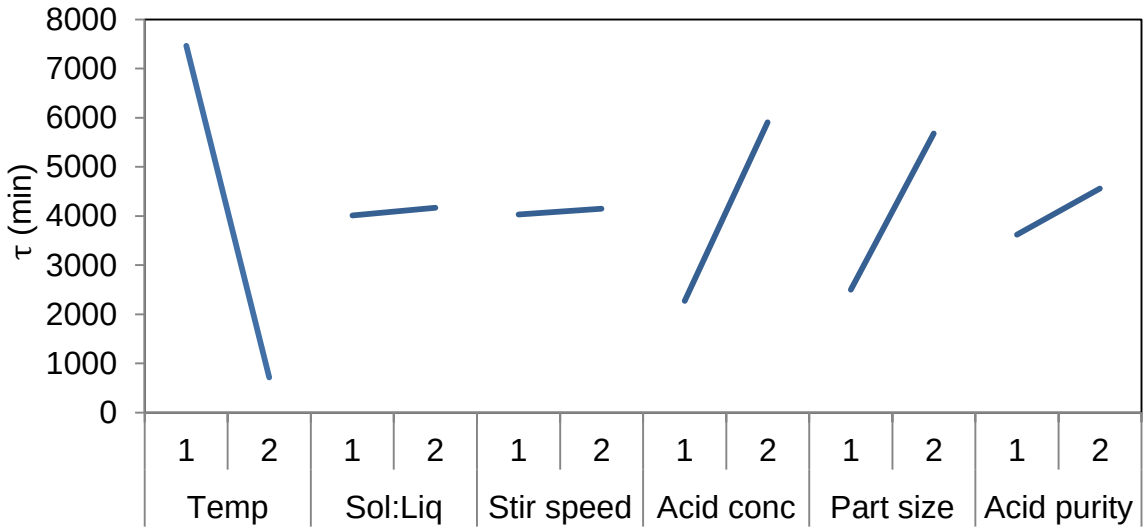

Figure 28: Main effects of τ for the overall ion leaching with Nitric acid

Table 28: ANOVA analysis of τ for overall leaching with nitric acid

Parameter	Variance	F	P
T	$9x10^7$	42.22	64.29
SL	47368	0.022	0.03
SS	28923	0.013	0.02
AC	$3x10^7$	12.26	18.67
PS	$2x10^7$	9.352	14.24
AP	$2x10^6$	0.807	1.23
Error	$2x10^6$	1	1.52

Again τ does not follow the relation as in literature therefore an empirical equation describing τ as a function of temperature, acid concentration and particle size can be derived from the analysis above allowing for the calculation of a pseudo τ value. The empirical equation is given in Equation 43.

$$\tau = -337.4T + 132.2AC + 18.05PS + 117711 \quad (43)$$

This equation is limited by the fact that τ cannot be negative therefore nonlinear behaviour is expected as τ becomes smaller. The Information gathered in section 4 is summarized in Table 29.

Table 29: Summary of results and models

	Hydrochloric acid		Nitric acid	
	Potassium leaching	Overall leaching	Potassium leaching	Overall leaching
Average conversion	0.4089	0.4440	0.7035	0.5068
Parameters affecting conversion	*T, AC* and *AP*	*T* and *AP*	*T* and *AC*	*T* and *AC*
Average selectivity	20.42	-	35.34	-
Parameters affecting selectivity	*T, SL, SS, PS* and *AP*	-	*T*	-
Best fitting model	Ash diffusion limited flat plate shrinking core ($X^2 = \frac{t}{\tau}$)	Empirical model 1 $\frac{dX}{dt}=k(4-X)(1-X)$	Ash diffusion limited flat plate shrinking core ($X^2 = \frac{t}{\tau}$)	Ash diffusion limited flat plate shrinking core ($X^2 = \frac{t}{\tau}$)

5. Conclusion

It was found that nitric acid performed the best as a leaching agent for phlogopite. Nitric acid did not only achieve the best conversion with regards to ions leached in a set time but also had the best potassium selectivity, which is an important characteristic for this study. It was found that temperature play the largest role in conversion as well as selectivity for all acids used. The leaching of potassium is best described by the ash diffusion rate limited flat plate shrinking core model for both hydrochloric as well as nitric acid. This model also best predicted the overall ion leaching of nitric acid but the overall leaching of hydrochloric acid was best described by an empirical leaching model. The fitted models did not follow literature with regard to which parameters impact the models therefore pseudo relations were developed to best describe the relationship between equation constants and the relative parameters. Sulphuric, citric acid had limited success whereas acetic acid was completely inefficient at leaching phlogopite. It would be recommended that further studies be conducted with the focus on the parameters identified as playing a substantial role. These studies should investigate potential nonlinear relationships of parameters as well as possible interactions.

6. References

Ayanda, OS, Adekola, FA, Baba, AA, Fatoki, OS and Ximba, BJ (2011) "Comparative study of the kinetics of dissolution of laterite in some acidic media" *Journal of Minerals & Materials Characterization & Engineering*, 10(15), 1457-1472

Barabaszova, KC, Valaskova, M (2013) "Characterization of vermiculite particles after different milling techniques" *Powder Technology*, 239, 277–283

Candido, D, Mathur, GP (1974) "An investigation into the kinetics of reaction between fluorspar and sulfuric acid" *Industrial & Engineering Chemistry Process Design and Development*, 13(1)

Clemency, CV, Lin, F (1981) "Dissolution of phlogopite. II. Open system using an ion-exchange resin" *Clay and Clay Minerals*, 29(2), 107-112

Fogler, HS (2004) *Elements of Chemical Reaction Engineering,* Prentice-Hall of India, New Delhi.

Harkonen, MA, Keiski, RL (1984) "Porosity and surface area of acid leached phlogopite: The effect of leaching conditions and thermal treatment" *Colloids and surfaces,* 11, 323 - 339

Kaviratna, H, Pinnavaia, TJ (1994) "Acid hydrolysis of octahedral Mg 2^{+} sites in 2:1 layered silicates: An assessment of edge attack and gallery access mechanism" *Clay and Clay Minerals*, 42(6), 717-723

Khalighi, M, Minkkinen, P (1989) “The evaporation of potassium from phlogopite” *Journal of thermal analysis*, 35 379-390

Kuwahara, Y, Aoki, Y (1995) “Dissolution process of phlogopite in acid solutions” *Clay and Clay Minerals*, 43(1), 39-50.

Levenspiel, O (1999) *Chemical Reaction Engineering Third Edition*, John Wiley & Sons, New York.

Mamy, J (1969) “Extraction of interlayer K from phlogopite specific effects of cations role of Na and H concentrations in extraction solutions” *Clay and Clay Minerals*, 18(1), 157-163.

Maqueda, C, Romero, AS, Morillo, E, Pérez-Rodríguez, JL (2007) “Effect of grinding on the preparation of porous materials by acid-leached vermiculite” *Journal of Physics and Chemistry of Solids,* 68, 1220-1224.

Murdoch University (2006) “Hydrometallurgy Theory and Practice” *Minerals Council of Australia*

Novak, I, Cicel, B (1978) “Dissolution of smectites in hydrochloric acid: Dissolution rate as a function of crystallochemical composition” *Clays Clay Min,* 26, 341 – 344

Okada, K, Arimitsu, N, Kameshima, Y, Nakajima, A, MacKenzie, KJD (2005) “Preparation of porous silica from chlorite by selective acid leaching” *Applied Clay Science*, 30, 116-124.

Okada, K, Arimitsu, N, Kameshima, Y, Nakajima, A, MacKenzie, KJD (2006) “Solid acidity of 2:1 type clay minerals activated by selective leaching” *Applied Clay Science*, 31, 185-193.

Ross, GJ, Rich, CI (1973) “Effect of particle thickness on potassium exchange from phlogopite” *Clays and Clay Minerals,* 21, 77-81

Scott, AD, Smith, SJ (1966) “Susceptibility of interlayer potassium in micas to exchange with sodium” *Iowa Agricultural and Home Economics Experiment Station,* J-5216, 69- 81

Sohn, HY, Wadsworth, ME, (1979) *Rate Processes of Extractive Metallurgy,* Plenum Press, New York.

Temuujin, J, Okada, K, MacKenzie, KJD (2003) “Preparation of porous silica from vermiculite by selective leaching” *Applied Clay Science*, 22, 187-195.

Welty, JR, Wicks, CE, Wilson, RE, Rorrer, GL (2008) *Fundamentals of Momentum, Heat, and Mass Transfer 5 edition,* John Wiley & Sons, Inc, Hoboken.

Williams PJ, Cloete TE (2010) “The production and use of citric acid for the removal of potassium from the iron ore concentrate of the Sishen Iron Ore Mine”, J Sci. 2010;106(3/4), Art. #158, 5 pages.

Appendix A1

Hydrochloric Acid K concentration

Time (min)	C_K (mg/l)							
	Exp 1	Exp 2	Exp 3	Exp 4	Exp 5	Exp 6	Exp 7	Exp 8
30	1092.2		1512.7	1038.6	974.8	389.2	462.2	1756.0
60	1127.2	863.3	1551.9	1215.3	1195.4	896.7	686.8	2907.7
90	1211.8	1007.0	1734.2	1340.5	1571.4	1386.3	1039.9	4313.0
120	1351.3	843.6	1771.5	992.3	2015.7	1882.9	1564.7	4665.2
180	1433.6	910.2	1899.8	1787.3	2930.9	2643.0	2609.7	5437.2
240	1944.5	1035.4	2125.8	2257.6	3586.5	2817.2	4197.2	6277.0
360	2198.0	929.6	2196.4	2957.8	4322.7	2623.5	6133.4	6459.9

Hydrochloric Acid Mg concentration

Time (min)	C_{Mg} (mg/l)							
	Exp 1	Exp 2	Exp 3	Exp 4	Exp 5	Exp 6	Exp 7	Exp 8
30	2937.8	265.6	4454.0	1777.3	2070.8	3363.3	2210.1	8476.0
60	3218.5	953.0	5114.7	2573.6	2863.3	4851.2	2911.4	11823.4
90	3604.2	1163.9	5620.9	3047.2	4088.4	6397.7	3973.7	14942.4
120	3893.9	1270.3	6182.3	1492.0	5379.8	7325.2	5271.9	16433.5
180	4220.9	1467.8	6469.8	4590.3	8062.0	9038.9	9061.3	17942.7
240	5376.6	1650.9	6944.8	6388.6	10120.5	9431.4	13020.7	20219.0
360	6248.6	1909.1	7302.1	8531.2	12020.4	9128.1	17395.5	19885.3

Hydrochloric Acid Fe concentration

Time (min)	C_{Fe} (mg/l)							
	Exp 1	Exp 2	Exp 3	Exp 4	Exp 5	Exp 6	Exp 7	Exp 8
30	1105.0		930.5	798.9	872.0	1085.1	594.4	3537.5
60	1237.4	397.1	1022.5	1105.6	1208.8	1773.3	925.9	4758.5
90	1412.9	526.0	1400.3	1337.0	1689.2	2289.1	1402.6	5966.2
120	1553.0	544.4	1475.6	738.5	2198.2	2785.6	1995.8	6462.7
180	1742.6	628.0	1985.5	2177.0	3171.5	3402.9	3166.2	6918.9
240	2318.3	769.7	2088.9	2608.2	3718.2	3557.7	4446.1	7816.1
360	2610.9	814.7	2284.2	3459.0	4265.5	3384.0	6025.7	7885.5

Hydrochloric Acid Al concentration

Time (min)	C_{Al} (mg/l)							
	Exp 1	Exp 2	Exp 3	Exp 4	Exp 5	Exp 6	Exp 7	Exp 8
30	535.9		444.2	798.9	705.2	652.6	488.8	1696.5
60	604.1	204.6	651.2	1105.6	958.8	1155.6	700.4	2767.3
90	706.7	268.8	769.5	1337.0	1373.3	1629.3	1066.9	3894.7
120	797.0	285.0	897.2	738.5	1819.5	2002.9	1443.1	4280.9
180	930.9	354.3	1093.2	2177.0	2742.2	2511.1	2612.6	4817.2
240	1321.4	440.2	1241.4	2608.2	3363.7	2640.6	3869.9	5503.2
360	1597.3	508.4	1381.0	3459.0	3965.5	2541.2	5369.7	5527.6

Nitric Acid K concentration

Time (min)	C_K (mg/l)							
	Exp 1	Exp 2	Exp 3	Exp 4	Exp 5	Exp 6	Exp 7	Exp 8
30	1678.2	1188.5	3869.1	2065.6	2430.5	2006.5	3607.0	749.7
60	2613.6	1568.3	4875.3	3047.2	2492.8	1981.0	3711.6	3780.2
90	2882.3	1879.6		3347.6	2864.2	2547.1	4461.0	4407.2
120	2962.6	1938.9	6983.6	3720.5	3242.9	2886.0	5505.0	4150.8
180	3134.0	1940.9	7198.2	4101.9	1456.8	3170.8		5148.0
240	3173.1	2116.0	6416.6	4385.0	4766.3	4048.0	9621.9	6528.3
360	3367.8	2238.4	7202.8	4977.9	5699.6	4860.7	12474.9	8208.1

Nitric Acid Mg concentration

Time (min)	C_{Mg} (mg/l)							
	Exp 1	Exp 2	Exp 3	Exp 4	Exp 5	Exp 6	Exp 7	Exp 8
30	944.6		3174.4	1071.1	2443.7	2838.0	2815.3	526.9
60	2097.3	473.3	3740.7	1532.2	3130.8	3575.5	3708.1	7782.6
90	2725.6	188.4		1649.4	4003.0	4283.4	4955.5	8966.1
120	3319.0	461.8	5436.3	2236.0	5494.6	5159.7	6912.8	9213.1
180	4052.1	845.7	5543.0	2489.5	2320.9	6384.5		12051.2
240	4144.3	658.2	5940.1	3222.8	9895.2	8403.2	16015.1	14940.9
360	4596.0	1591.3	6919.5	4424.0	12821.4	11183.3	24083.4	21229.5

Nitric Acid Fe concentration

Time (min)	C_{Fe} (mg/l)							
	Exp 1	Exp 2	Exp 3	Exp 4	Exp 5	Exp 6	Exp 7	Exp 8
30	352.8	559.6	577.5	394.1	705.5	470.8	570.9	57.9
60	675.6	574.4	738.2	510.7	1075.7	799.5	902.7	1846.8
90	987.8	585.3		606.9	1381.5	1073.7	1396.2	2301.3
120	1110.8	611.3	1135.3	757.1	1957.7	1380.6	2399.9	2562.2
180	1486.0	644.8	1572.4	1026.6	733.4	1785.5		3600.9
240	1540.4	754.3	1538.2	1032.5	3333.0	2518.6	5058.7	4518.4
360	1678.6	770.3	1927.9	1571.1	4248.0	3588.9	7867.0	6873.5

Nitric Acid Al concentration

Time (min)	C_{Al} (mg/l)							
	Exp 1	Exp 2	Exp 3	Exp 4	Exp 5	Exp 6	Exp 7	Exp 8
30	377.9	166.3	290.3	377.9	764.0	508.3	714.2	211.6
60	658.7	210.6	486.8	489.7	1018.6	741.6	994.8	1614.9
90	866.1	261.0		550.4	1328.8	985.1	1421.2	2088.0
120	977.7	271.6	987.0	676.8	1750.9	1265.3	2127.7	2200.4
180	1216.8	349.7	1120.7	815.2		1680.3		3056.7
240	1298.1	431.3	1205.5	956.1	3166.6	2316.7	5205.7	4069.0
360	1380.5	515.3	1589.6	1302.1	4057.4	3142.3	7905.1	6077.9

Appendix A2

Hydrochloric Acid K conversion

Time (min)	Exp 1	Exp 2	Exp 3	Exp 4	Exp 5	Exp 6	Exp 7	Exp 8
30	0.189		0.131	0.090	0.168	0.067	0.040	0.152
60	0.195	0.149	0.134	0.105	0.206	0.155	0.059	0.251
90	0.209	0.174	0.150	0.116	0.271	0.239	0.090	0.372
120	0.233	0.146	0.153	0.086	0.348	0.325	0.135	0.403
180	0.248	0.157	0.164	0.154	0.506	0.456	0.225	0.469
240	0.336	0.179	0.184	0.195	0.619	0.486	0.362	0.542
360	0.379	0.160	0.190	0.255	0.746	0.453	0.529	0.558

Hydrochloric Acid overall conversion

Time (min)	Exp 1	Exp 2	Exp 3	Exp 4	Exp 5	Exp 6	Exp 7	Exp 8
30	0.180		0.116	0.070	0.146	0.174	0.059	0.245
60	0.196	0.077	0.132	0.095	0.197	0.275	0.083	0.352
90	0.220	0.094	0.151	0.112	0.276	0.371	0.118	0.461
120	0.240	0.093	0.163		0.361	0.443	0.163	0.504
180	0.264	0.106	0.181	0.170	0.535	0.557	0.276	0.556
240	0.347	0.123	0.196	0.219	0.658	0.584	0.404	0.630
360	0.401	0.132	0.208	0.291	0.778	0.560	0.553	0.629

Nitric acid K conversion

Time (min)	Exp 1	Exp 2	Exp 3	Exp 4	Exp 5	Exp 6	Exp 7	Exp 8
30	0.290	0.205	0.334	0.178	0.420	0.346	0.311	0.065
60	0.451	0.271	0.421	0.263	0.430	0.342	0.320	0.326
90	0.498	0.325		0.289	0.495	0.440	0.385	0.380
120	0.512	0.335	0.603	0.321	0.560	0.498	0.475	0.358
180	0.541	0.335	0.621	0.354	0.252	0.547		0.444
240	0.548	0.365	0.554	0.379	0.823	0.699	0.831	0.564
360	0.581	0.386	0.622	0.430	0.984	0.839	1.077	0.709

Nitric acid overall conversion

Time (min)	Exp 1	Exp 2	Exp 3	Exp 4	Exp 5	Exp 6	Exp 7	Exp 8
30	0.106	0.058	0.125	0.062	0.201	0.184	0.122	0.024
60	0.191	0.089	0.156	0.088	0.244	0.225	0.148	0.238
90	0.236	0.092		0.097	0.303	0.281	0.194	0.281
120	0.265	0.104	0.230	0.117	0.394	0.339	0.268	0.287
180	0.313	0.120	0.244	0.134		0.412		0.378
240	0.322	0.125	0.239	0.152	0.670	0.547	0.568	0.476
360	0.349	0.162	0.279	0.194	0.849	0.721	0.828	0.671

Appendix B

Hydrochloric Acid K leaching Model fits

Flat plate ash diffusion rate limited shrinking core

Time (min)	X^2							
	Exp 1	Exp 2	Exp 3	Exp 4	Exp 5	Exp 6	Exp 7	Exp 8
30	0.036	0.002	0.017	0.008	0.028	0.005	0.002	0.023
60	0.038	0.022	0.018	0.011	0.043	0.024	0.004	0.063
90	0.044	0.030	0.022	0.013	0.074	0.057	0.008	0.139
120	0.054	0.021	0.023	0.007	0.121	0.106	0.018	0.162
180	0.061	0.025	0.027	0.024	0.256	0.208	0.051	0.220
240	0.113	0.032	0.034	0.038	0.383	0.237	0.131	0.294
360	0.144	0.026	0.036	0.065	0.557	0.205	0.280	0.311

Spherical ash diffusion rate limited shrinking core

Time (min)	$1 - 2(1 - x) - 3(1-x)^{2/3}$							
	Exp 1	Exp 2	Exp 3	Exp 4	Exp 5	Exp 6	Exp 7	Exp 8
30	0.0043	0.0003	0.002	0.0009	0.0034	0.0005	0.0002	0.0027
60	0.0046	0.0026	0.0021	0.0013	0.0052	0.0029	0.0004	0.0079
90	0.0054	0.0036	0.0027	0.0016	0.0094	0.0072	0.0009	0.0187
120	0.0068	0.0025	0.0028	0.0008	0.0161	0.0139	0.0022	0.0223
180	0.0077	0.003	0.0032	0.0028	0.0378	0.0297	0.0063	0.0317
240	0.0149	0.0039	0.0041	0.0046	0.0618	0.0344	0.0176	0.0445
360	0.0195	0.0031	0.0044	0.0082	0.1017	0.0291	0.0421	0.0477

Spherical reaction rate limited shrinking core

Time (min)	$1 – (1 - X)^{1/3}$							
	Exp 1	Exp 2	Exp 3	Exp 4	Exp 5	Exp 6	Exp 7	Exp 8
30	0.0673	-0.016	0.0456	0.0308	0.0596	0.0229	0.0135	0.0533
60	0.0696	0.0524	0.0468	0.0363	0.0742	0.0545	0.0202	0.0918
90	0.0753	0.0617	0.0526	0.0402	0.1001	0.0872	0.0309	0.1438
120	0.0847	0.0511	0.0538	0.0294	0.1329	0.1228	0.0472	0.1579
180	0.0904	0.0554	0.058	0.0543	0.2095	0.1838	0.0816	0.1904
240	0.1275	0.0635	0.0653	0.0697	0.2752	0.1992	0.1393	0.2291
360	0.1471	0.0566	0.0677	0.0936	0.367	0.1822	0.2222	0.2381

Spherical external mass transfer limited shrinking core

Time (min)	$1 - (1 - X)^{0.5}$							
	Exp 1	Exp 2	Exp 3	Exp 4	Exp 5	Exp 6	Exp 7	Exp 8
30	0.0992	-0.024	0.0676	0.0459	0.088	0.0342	0.0202	0.0789
60	0.1026	0.0775	0.0694	0.0539	0.1092	0.0807	0.0301	0.1346
90	0.1107	0.0911	0.0779	0.0596	0.1464	0.1278	0.0459	0.2077
120	0.1244	0.0757	0.0796	0.0438	0.1925	0.1785	0.07	0.2272
180	0.1325	0.0819	0.0857	0.0804	0.2972	0.2627	0.1198	0.2716
240	0.185	0.0938	0.0964	0.1027	0.3829	0.2833	0.2015	0.3232
360	0.2123	0.0838	0.0998	0.1371	0.4963	0.2604	0.3141	0.3349

Power law first order

Time (min)	Ln(C)							
	Exp 1	Exp 2	Exp 3	Exp 4	Exp 5	Exp 6	Exp 7	Exp 8
30	6.9959		7.3217	6.9456	6.8822	5.9641	6.136	7.4708
60	7.0275	6.7608	7.3472	7.1027	7.0862	6.7987	6.532	7.9751
90	7.0999	6.9147	7.4583	7.2008	7.3597	7.2344	6.9469	8.3694
120	7.2088	6.7377	7.4796	6.9	7.6087	7.5406	7.3554	8.4479
180	7.2679	6.8137	7.5495	7.4885	7.9831	7.8797	7.867	8.601
240	7.5728	6.9425	7.6619	7.7221	8.1849	7.9435	8.3422	8.7446
360	7.6953	6.8348	7.6946	7.9922	8.3716	7.8723	8.7215	8.7734

Power law second order

Time (min)	1/C							
	Exp 1	Exp 2	Exp 3	Exp 4	Exp 5	Exp 6	Exp 7	Exp 8
30	0.0009	-0.004	0.0007	0.001	0.001	0.0026	0.0022	0.0006
60	0.0009	0.0012	0.0006	0.0008	0.0008	0.0011	0.0015	0.0003
90	0.0008	0.001	0.0006	0.0007	0.0006	0.0007	0.001	0.0002
120	0.0007	0.0012	0.0006	0.001	0.0005	0.0005	0.0006	0.0002
180	0.0007	0.0011	0.0005	0.0006	0.0003	0.0004	0.0004	0.0002
240	0.0005	0.001	0.0005	0.0004	0.0003	0.0004	0.0002	0.0002
360	0.0005	0.0011	0.0005	0.0003	0.0002	0.0004	0.0002	0.0002

Power law third order

Time (min)	$1/2C^2$							
	Exp 1	Exp 2	Exp 3	Exp 4	Exp 5	Exp 6	Exp 7	Exp 8
30	4E-07	6E-06	2E-07	5E-07	5E-07	3E-06	2E-06	2E-07
60	4E-07	7E-07	2E-07	3E-07	3E-07	6E-07	1E-06	6E-08
90	3E-07	5E-07	2E-07	3E-07	2E-07	3E-07	5E-07	3E-08
120	3E-07	7E-07	2E-07	5E-07	1E-07	1E-07	2E-07	2E-08
180	2E-07	6E-07	1E-07	2E-07	6E-08	7E-08	7E-08	2E-08
240	1E-07	5E-07	1E-07	1E-07	4E-08	6E-08	3E-08	1E-08
360	1E-07	6E-07	1E-07	6E-08	3E-08	7E-08	1E-08	1E-08

Empirical model 1

Time (min)	$X_{Predicted}$							
	Exp 1	Exp 2	Exp 3	Exp 4	Exp 5	Exp 6	Exp 7	Exp 8
30	0.1886	0	0.1306	0.0897	0.1683	0.0672	0.0399	0.1516
60	0.2074	0.1491	0.1396	0.1057	0.2479	0.1368	0.0958	0.2146
90	0.2257	0.1532	0.1485	0.1213	0.3184	0.2002	0.147	0.2709
120	0.2434	0.1574	0.1573	0.1366	0.3811	0.2579	0.1939	0.3215
180	0.278	0.1656	0.1746	0.1663	0.4931	0.3633	0.2804	0.413
240	0.3107	0.1737	0.1914	0.1945	0.5819	0.4512	0.354	0.4878
360	0.3725	0.1898	0.2239	0.2481	0.7248	0.5991	0.4803	0.6123

Empirical model 2

Time (min)	$X_{Predicted}$							
	Exp 1	Exp 2	Exp 3	Exp 4	Exp 5	Exp 6	Exp 7	Exp 8
30	0.1886	0	0.1306	0.0897	0.1683	0.0672	0.0399	0.1516
60	0.2069	0.1491	0.1395	0.1054	0.2388	0.1305	0.092	0.2073
90	0.2249	0.1532	0.1483	0.1208	0.3041	0.1899	0.1409	0.259
120	0.2426	0.1573	0.157	0.136	0.3645	0.2457	0.1868	0.307
180	0.2772	0.1655	0.1743	0.1656	0.4763	0.3506	0.2732	0.3962
240	0.3104	0.1737	0.1911	0.1942	0.5716	0.4428	0.3495	0.4733
360	0.3742	0.1898	0.224	0.249	0.7338	0.6052	0.485	0.6073

Empirical model 3

Time (min)	$X_{Predicted}$							
	Exp 1	Exp 2	Exp 3	Exp 4	Exp 5	Exp 6	Exp 7	Exp 8
30	0.1886		0.1306	0.0897	0.1683	0.0672	0.0399	0.1516
60	0.2117	0.1491	0.1418	0.1133	0.3095	0.2422	0.1994	0.2731
90	0.2318	0.1536	0.152	0.1315	0.3751	0.2827	0.2254	0.3301
120	0.2498	0.158	0.1613	0.1468	0.4249	0.3158	0.2476	0.3734
180	0.2824	0.1665	0.1787	0.1737	0.5073	0.3728	0.2867	0.4449
240	0.3103	0.1745	0.1941	0.1956	0.5686	0.4178	0.3187	0.498
360	0.3593	0.1896	0.2218	0.2334	0.6677	0.4935	0.3735	0.5842

Empirical model 4

Time (min)	(1 - X) + XlnX							
	Exp 1	Exp 2	Exp 3	Exp 4	Exp 5	Exp 6	Exp 7	Exp 8
30	0.4968		0.6036	0.6941	0.5318	0.7514	0.8316	0.5624
60	0.4869	0.5672	0.5967	0.6585	0.4679	0.5564	0.7732	0.402
90	0.4635	0.522	0.566	0.6347	0.3748	0.4184	0.6938	0.2598
120	0.4271	0.5737	0.5599	0.7038	0.2846	0.3096	0.5945	0.231
180	0.4069	0.552	0.5395	0.5573	0.1493	0.1857	0.4389	0.1756
240	0.2978	0.5135	0.5053	0.4864	0.084	0.163	0.2698	0.1261
360	0.2528	0.5459	0.4951	0.3961	0.0353	0.1883	0.1338	0.1167

Hydrochloric Acid overall leaching Model fits

Flat plate ash diffusion rate limited shrinking core

Time (min)	X^2							
	Exp 1	Exp 2	Exp 3	Exp 4	Exp 5	Exp 6	Exp 7	Exp 8
30	0.032		0.014	0.005	0.021	0.030	0.004	0.060
60	0.038	0.006	0.017	0.009	0.039	0.075	0.007	0.124
90	0.048	0.009	0.023	0.012	0.076	0.137	0.014	0.212
120	0.058	0.009	0.027		0.131	0.196	0.026	0.254
180	0.070	0.011	0.033	0.029	0.287	0.310	0.076	0.309
240	0.120	0.015	0.039	0.048	0.433	0.341	0.163	0.397
360	0.161	0.017	0.043	0.085	0.605	0.313	0.306	0.396

Spherical ash diffusion rate limited shrinking core

Time (min)	$1 - 2(1 - x) - 3(1-x)^{2/3}$							
	Exp 1	Exp 2	Exp 3	Exp 4	Exp 5	Exp 6	Exp 7	Exp 8
30	0.004	0.000	0.002	0.001	0.003	0.004	0.000	0.008
60	0.005	0.001	0.002	0.001	0.005	0.010	0.001	0.017
90	0.006	0.001	0.003	0.001	0.010	0.018	0.002	0.030
120	0.007	0.001	0.003		0.017	0.028	0.003	0.037
180	0.009	0.001	0.004	0.003	0.043	0.048	0.010	0.047
240	0.016	0.002	0.005	0.006	0.072	0.053	0.022	0.065
360	0.022	0.002	0.005	0.011	0.115	0.048	0.047	0.064

Spherical reaction rate limited shrinking core

Time (min)	$1 – (1 - X)^{1/3}$							
	Exp 1	Exp 2	Exp 3	Exp 4	Exp 5	Exp 6	Exp 7	Exp 8
30	0.064	0.000	0.040	0.024	0.051	0.062	0.020	0.089
60	0.070	0.026	0.046	0.033	0.071	0.102	0.028	0.135
90	0.079	0.032	0.053	0.039	0.102	0.143	0.041	0.186
120	0.088	0.032	0.058		0.139	0.177	0.057	0.208
180	0.097	0.037	0.064	0.060	0.225	0.238	0.102	0.237
240	0.132	0.043	0.070	0.079	0.301	0.254	0.159	0.282
360	0.157	0.046	0.075	0.108	0.395	0.239	0.235	0.282

Spherical external mass transfer limited shrinking core

Time (min)	$1 – (1 – X)^{0.5}$							
	Exp 1	Exp 2	Exp 3	Exp 4	Exp 5	Exp 6	Exp 7	Exp 8
30	0.094	0.000	0.060	0.036	0.076	0.091	0.030	0.131
60	0.103	0.039	0.068	0.049	0.104	0.148	0.042	0.195
90	0.117	0.048	0.078	0.058	0.149	0.207	0.061	0.266
120	0.128	0.048	0.085	0.000	0.201	0.254	0.085	0.296
180	0.142	0.055	0.095	0.089	0.318	0.335	0.149	0.334
240	0.192	0.064	0.104	0.117	0.415	0.355	0.228	0.392
360	0.226	0.068	0.110	0.158	0.529	0.336	0.331	0.391

Power law first order

Time (min)	Ln(C)							
	Exp 1	Exp 2	Exp 3	Exp 4	Exp 5	Exp 6	Exp 7	Exp 8
30	8.643		8.901	8.392	8.439	8.611	8.231	9.646
60	8.730	7.791	9.029	8.700	8.737	9.068	8.561	10.010
90	8.844	7.995	9.162	8.862	9.074	9.368	8.920	10.279
120	8.935	7.987	9.242	8.284	9.343	9.547	9.238	10.369
180	9.027	8.120	9.346	9.281	9.735	9.775	9.767	10.466
240	9.302	8.268	9.426	9.537	9.942	9.823	10.148	10.592
360	9.446	8.334	9.485	9.820	10.109	9.780	10.461	10.591

Power law second order

Time (min)	1/C							
	Exp 1	Exp 2	Exp 3	Exp 4	Exp 5	Exp 6	Exp 7	Exp 8
30	1.76E-04	-2.93E-03	1.36E-04	2.27E-04	2.16E-04	1.82E-04	2.66E-04	6.47E-05
60	1.62E-04	4.14E-04	1.20E-04	1.67E-04	1.61E-04	1.15E-04	1.91E-04	4.49E-05
90	1.44E-04	3.37E-04	1.05E-04	1.42E-04	1.15E-04	8.55E-05	1.34E-04	3.43E-05
120	1.32E-04	3.40E-04	9.68E-05	2.52E-04	8.76E-05	7.14E-05	9.73E-05	3.14E-05
180	1.20E-04	2.98E-04	8.73E-05	9.32E-05	5.91E-05	5.68E-05	5.73E-05	2.85E-05
240	9.12E-05	2.57E-04	8.06E-05	7.21E-05	4.81E-05	5.42E-05	3.92E-05	2.51E-05
360	7.90E-05	2.40E-04	7.60E-05	5.43E-05	4.07E-05	5.66E-05	2.86E-05	2.52E-05

Power law third order

Time (min)	$1/2C^2$							
	Exp 1	Exp 2	Exp 3	Exp 4	Exp 5	Exp 6	Exp 7	Exp 8
30	1.55E-08	4.29E-06	9.28E-09	2.57E-08	2.34E-08	1.66E-08	3.55E-08	2.09E-09
60	1.31E-08	8.55E-08	7.19E-09	1.39E-08	1.29E-08	6.64E-09	1.83E-08	1.01E-09
90	1.04E-08	5.68E-08	5.51E-09	1.00E-08	6.57E-09	3.65E-09	8.93E-09	5.90E-10
120	8.67E-09	5.77E-08	4.69E-09	3.19E-08	3.84E-09	2.55E-09	4.74E-09	4.93E-10
180	7.21E-09	4.43E-08	3.81E-09	4.34E-09	1.75E-09	1.61E-09	1.64E-09	4.05E-10
240	4.16E-09	3.29E-08	3.25E-09	2.60E-09	1.16E-09	1.47E-09	7.67E-10	3.15E-10
360	3.12E-09	2.89E-08	2.89E-09	1.48E-09	8.28E-10	1.60E-09	4.10E-10	3.16E-10

Empirical model 1

Time (min)	$X_{Predicted}$							
	Exp 1	Exp 2	Exp 3	Exp 4	Exp 5	Exp 6	Exp 7	Exp 8
30	0.180	0.000	0.116	0.070	0.146	0.174	0.059	0.245
60	0.202	0.077	0.128	0.093	0.239	0.248	0.115	0.304
90	0.225	0.084	0.139	0.114	0.319	0.314	0.166	0.358
120	0.246	0.091	0.150	0.136	0.390	0.373	0.214	0.407
180	0.288	0.106	0.171	0.177	0.514	0.479	0.303	0.496
240	0.326	0.120	0.192	0.216	0.609	0.565	0.380	0.569
360	0.399	0.148	0.233	0.290	0.758	0.705	0.514	0.693

Empirical model 2

Time (min)	$X_{Predicted}$							
	Exp 1	Exp 2	Exp 3	Exp 4	Exp 5	Exp 6	Exp 7	Exp 8
30	0.180	0.000	0.116	0.070	0.146	0.174	0.059	0.245
60	0.202	0.077	0.127	0.092	0.227	0.240	0.111	0.296
90	0.224	0.084	0.138	0.113	0.301	0.301	0.159	0.345
120	0.245	0.091	0.149	0.135	0.369	0.358	0.206	0.390
180	0.286	0.106	0.171	0.176	0.494	0.464	0.294	0.476
240	0.326	0.120	0.192	0.215	0.598	0.555	0.373	0.551
360	0.401	0.148	0.233	0.291	0.771	0.712	0.517	0.685

Empirical model 3

Time (min)	$X_{Predicted}$							
	Exp 1	Exp 2	Exp 3	Exp 4	Exp 5	Exp 6	Exp 7	Exp 8
30	0.180		0.116	0.070	0.146	0.174	0.059	0.245
60	0.209	0.077	0.132	0.111	0.322	0.301	0.205	0.336
90	0.234	0.087	0.146	0.136	0.388	0.365	0.241	0.396
120	0.256	0.095	0.158	0.156	0.438	0.413	0.271	0.443
180	0.294	0.111	0.180	0.190	0.521	0.494	0.322	0.522
240	0.326	0.125	0.199	0.217	0.583	0.554	0.362	0.581
360	0.382	0.148	0.233	0.262	0.683	0.651	0.431	0.678

Empirical model 4

Time (min)	(1 - X) + XlnX							
	Exp 1	Exp 2	Exp 3	Exp 4	Exp 5	Exp 6	Exp 7	Exp 8
30	0.512		0.634	0.744	0.572	0.522	0.773	0.411
60	0.485	0.727	0.601	0.681	0.483	0.370	0.711	0.280
90	0.448	0.684	0.564	0.643	0.368	0.262	0.629	0.182
120	0.417	0.686	0.540		0.271	0.196	0.542	0.151
180	0.385	0.655	0.509	0.529	0.130	0.117	0.368	0.118
240	0.286	0.618	0.484	0.448	0.067	0.102	0.230	0.079
360	0.233	0.601	0.465	0.349	0.027	0.115	0.119	0.079

Nitric Acid K leaching Model fits

Flat plate ash diffusion rate limited shrinking core

Time (min)	X^2							
	Exp 1	Exp 2	Exp 3	Exp 4	Exp 5	Exp 6	Exp 7	Exp 8
30	0.084	0.042	0.112	0.032	0.176	0.120	0.097	0.004
60	0.204	0.073	0.177	0.069	0.185	0.117	0.103	0.106
90	0.248	0.105		0.084	0.245	0.193	0.148	0.145
120	0.262	0.112	0.363	0.103	0.313	0.248	0.226	0.128
180	0.293	0.112	0.386	0.125		0.300		0.198
240	0.300	0.133	0.307	0.143	0.677	0.488	0.690	0.318
360	0.338	0.149	0.387	0.185	0.968	0.704	1.000	0.502

Spherical ash diffusion rate limited shrinking core

Time (min)	$1 - 2(1 - x) - 3(1-x)^{2/3}$							
	Exp 1	Exp 2	Exp 3	Exp 4	Exp 5	Exp 6	Exp 7	Exp 8
30	0.011	0.005	0.015	0.004	0.024	0.016	0.097	0.000
60	0.029	0.009	0.025	0.009	0.026	0.015	0.103	0.014
90	0.036	0.014		0.011	0.036	0.027	0.148	0.020
120	0.039	0.015	0.058	0.013	0.048	0.036	0.226	0.017
180	0.044	0.015	0.062	0.017		0.046		0.028
240	0.046	0.018	0.047	0.019	0.136	0.085	0.690	0.049
360	0.053	0.020	0.062	0.026	0.281	0.145	1.000	0.088

Spherical reaction rate limited shrinking core

Time (min)	$1 – (1 - X)^{1/3}$							
	Exp 1	Exp 2	Exp 3	Exp 4	Exp 5	Exp 6	Exp 7	Exp 8
30	0.108	0.074	0.127	0.063	0.166	0.132	0.117	0.022
60	0.181	0.100	0.166	0.097	0.171	0.130	0.121	0.123
90	0.205	0.123		0.107	0.203	0.176	0.150	0.148
120	0.212	0.127	0.265	0.121	0.239	0.205	0.193	0.137
180	0.229	0.127	0.277	0.136		0.232		0.178
240	0.232	0.141	0.236	0.147	0.438	0.330	0.447	0.241
360	0.252	0.150	0.277	0.171	0.748	0.456	1.425	0.337

Spherical external mass transfer limited shrinking core

Time (min)	$1 – (1 – X)^{0.5}$							
	Exp 1	Exp 2	Exp 3	Exp 4	Exp 5	Exp 6	Exp 7	Exp 8
30	0.157	0.108	0.184	0.906	0.762	0.808	0.830	0.967
60	0.259	0.146	0.239	0.858	0.755	0.811	0.824	0.821
90	0.291	0.178		0.843	0.711	0.748	0.784	0.787
120	0.301	0.184	0.370	0.824	0.663	0.708	0.724	0.801
180	0.323	0.185	0.385	0.804		0.673		0.745
240	0.328	0.203	0.332	0.788	0.421	0.549	0.412	0.661
360	0.353	0.217	0.385	0.755	0.126	0.401	1.000	0.540

Power law first order

Time (min)	Ln(C)							
	Exp 1	Exp 2	Exp 3	Exp 4	Exp 5	Exp 6	Exp 7	Exp 8
30	7.425	7.080	8.261	8.261	7.796	7.604	8.191	6.620
60	7.868	7.358	8.492	8.492	7.821	7.591	8.219	8.238
90	7.966	7.539			7.960	7.843	8.403	8.391
120	7.994	7.570	8.851	8.851	8.084	7.968	8.613	8.331
180	8.050	7.571	8.882	8.882		8.062		8.546
240	8.062	7.657	8.767	8.767	8.469	8.306	9.172	8.784
360	8.122	7.714	8.882	8.882	8.648	8.489	9.431	9.013

Power law second order

Time (min)	1/C							
	Exp 1	Exp 2	Exp 3	Exp 4	Exp 5	Exp 6	Exp 7	Exp 8
30	5.96E-04	8.41E-04	2.58E-04	4.84E-04	4.11E-04	4.98E-04	2.77E-04	1.33E-03
60	3.83E-04	6.38E-04	2.05E-04	3.28E-04	4.01E-04	5.05E-04	2.69E-04	2.65E-04
90	3.47E-04	5.32E-04		2.99E-04	3.49E-04	3.93E-04	2.24E-04	2.27E-04
120	3.38E-04	5.16E-04	1.43E-04	2.69E-04	3.08E-04	3.47E-04	1.82E-04	2.41E-04
180	3.19E-04	5.15E-04	1.39E-04	2.44E-04		3.15E-04		1.94E-04
240	3.15E-04	4.73E-04	1.56E-04	2.28E-04	2.10E-04	2.47E-04	1.04E-04	1.53E-04
360	2.97E-04	4.47E-04	1.39E-04	2.01E-04	1.75E-04	2.06E-04	8.02E-05	1.22E-04

Power law third order

Time (min)	$1/2C^2$							
	Exp 1	Exp 2	Exp 3	Exp 4	Exp 5	Exp 6	Exp 7	Exp 8
30	1.78E-07	3.54E-07	3.34E-08	1.17E-07	4.11E-04	4.98E-04	2.77E-04	1.33E-03
60	7.32E-08	2.03E-07	2.10E-08	5.38E-08	4.01E-04	5.05E-04	2.69E-04	2.65E-04
90	6.02E-08	1.42E-07		4.46E-08	3.49E-04	3.93E-04	2.24E-04	2.27E-04
120	5.70E-08	1.33E-07	1.03E-08	3.61E-08	3.08E-04	3.47E-04	1.82E-04	2.41E-04
180	5.09E-08	1.33E-07	9.65E-09	2.97E-08		3.15E-04		1.94E-04
240	4.97E-08	1.12E-07	1.21E-08	2.60E-08	2.10E-04	2.47E-04	1.04E-04	1.53E-04
360	4.41E-08	9.98E-08	9.64E-09	2.02E-08	1.75E-04	2.06E-04	8.02E-05	1.22E-04

Empirical model 1

Time (min)	$X_{Predicted}$							
	Exp 1	Exp 2	Exp 3	Exp 4	Exp 5	Exp 6	Exp 7	Exp 8
30	0.290	0.205	0.334	0.178	0.420	0.346	0.311	0.065
60	0.334	0.225	0.380	0.213	0.504	0.403	0.438	0.175
90	0.375	0.245	0.421	0.245	0.574	0.454	0.533	0.266
120	0.412	0.263	0.459	0.276	0.633	0.500	0.608	0.344
180	0.483	0.300	0.528	0.333	0.733	0.583	0.727	0.476
240	0.543	0.334	0.585	0.384	0.803	0.651	0.802	0.573
360	0.649	0.399	0.682	0.476	0.905	0.762	0.905	0.721

Empirical model 2

Time (min)	$X_{Predicted}$							
	Exp 1	Exp 2	Exp 3	Exp 4	Exp 5	Exp 6	Exp 7	Exp 8
30	0.290	0.205	0.334	0.178	0.420	0.346	0.311	0.065
60	0.329	0.224	0.375	0.211	0.497	0.397	0.422	0.160
90	0.366	0.243	0.413	0.242	0.565	0.445	0.514	0.244
120	0.402	0.261	0.448	0.272	0.626	0.489	0.591	0.319
180	0.470	0.297	0.515	0.329	0.734	0.573	0.722	0.452
240	0.531	0.331	0.574	0.382	0.818	0.645	0.813	0.558
360	0.642	0.397	0.677	0.478	0.944	0.769	0.943	0.730

Empirical model 3

Time (min)	$X_{Predicted}$							
	Exp 1	Exp 2	Exp 3	Exp 4	Exp 5	Exp 6	Exp 7	Exp 8
30	0.290	0.205	0.334	0.178	0.420	0.346	0.311	0.065
60	0.352	0.233	0.394	0.230	0.519	0.416	0.485	0.350
90	0.399	0.257	0.440	0.267	0.588	0.470	0.568	0.386
120	0.439	0.279	0.479	0.297	0.643	0.514	0.629	0.416
180	0.507	0.317	0.544	0.349	0.733	0.589	0.724	0.470
240	0.560	0.349	0.595	0.390	0.798	0.646	0.789	0.513
360	0.648	0.405	0.679	0.458	0.898	0.741	0.886	0.586

Empirical model 4

Time (min)	(1 - X) + XlnX							
	Exp 1	Exp 2	Exp 3	Exp 4	Exp 5	Exp 6	Exp 7	Exp 8
30	0.351	0.470	0.300	0.514	0.216	0.286	0.325	0.758
60	0.190	0.375	0.215	0.386	0.207	0.291	0.315	0.308
90	0.155	0.310		0.352	0.157	0.199	0.247	0.252
120	0.146	0.299	0.092	0.314	0.115	0.155	0.171	0.274
180	0.127	0.299	0.083	0.278		0.123		0.195
240	0.122	0.267	0.119	0.254	0.017	0.051	0.015	0.113
360	0.103	0.246	0.083	0.207	0.000	0.014	0.003	0.047

Nitric Acid overall leaching Model fits

Flat plate ash diffusion rate limited shrinking core

Time (min)	X^2							
	Exp 1	Exp 2	Exp 3	Exp 4	Exp 5	Exp 6	Exp 7	Exp 8
30	0.011	0.003	0.016	0.004	0.040	0.034	0.015	0.001
60	0.037	0.008	0.024	0.008	0.060	0.051	0.022	0.057
90	0.056	0.009		0.009	0.092	0.079	0.038	0.079
120	0.070	0.011	0.053	0.014	0.155	0.115	0.072	0.082
180	0.098	0.014	0.060	0.018		0.170		0.143
240	0.103	0.016	0.057	0.023	0.449	0.300	0.323	0.226
360	0.122	0.026	0.078	0.038	0.721	0.520	0.686	0.450

Spherical ash diffusion rate limited shrinking core

Time (min)	$1 - 2(1 - x) - 3(1-x)^{2/3}$							
	Exp 1	Exp 2	Exp 3	Exp 4	Exp 5	Exp 6	Exp 7	Exp 8
30	0.001	0.000	0.002	0.000	0.005	0.004	0.002	0.000
60	0.004	0.001	0.003	0.001	0.007	0.006	0.003	0.007
90	0.007	0.001		0.001	0.012	0.010	0.005	0.010
120	0.009	0.001	0.007	0.002	0.021	0.015	0.009	0.011
180	0.013	0.002	0.007	0.002		0.024		0.019
240	0.014	0.002	0.007	0.003	0.076	0.046	0.050	0.033
360	0.016	0.003	0.010	0.005	0.151	0.092	0.139	0.076

Spherical reaction rate limited shrinking core

Time (min)	$1 – (1 - X)^{1/3}$							
	Exp 1	Exp 2	Exp 3	Exp 4	Exp 5	Exp 6	Exp 7	Exp 8
30	0.037	0.020	0.044	0.021	0.072	0.066	0.042	0.008
60	0.068	0.031	0.055	0.030	0.089	0.081	0.052	0.087
90	0.086	0.032		0.034	0.113	0.104	0.069	0.104
120	0.098	0.036	0.084	0.041	0.154	0.129	0.099	0.107
180	0.118	0.042	0.089	0.047		0.162		0.146
240	0.121	0.044	0.087	0.053	0.309	0.232	0.244	0.194
360	0.133	0.057	0.103	0.069	0.468	0.347	0.444	0.310

Spherical external mass transfer limited shrinking core

Time (min)	$1 – (1 – X)^{0.5}$							
	Exp 1	Exp 2	Exp 3	Exp 4	Exp 5	Exp 6	Exp 7	Exp 8
30	0.055	0.029	0.065	0.031	0.106	0.097	0.063	0.012
60	0.101	0.046	0.081	0.045	0.131	0.120	0.077	0.127
90	0.126	0.047		0.050	0.165	0.152	0.102	0.152
120	0.143	0.053	0.123	0.060	0.222	0.187	0.145	0.156
180	0.171	0.062	0.131	0.069		0.233	0.000	0.211
240	0.176	0.065	0.128	0.079	0.426	0.327	0.343	0.276
360	0.193	0.085	0.151	0.102	0.612	0.472	0.586	0.426

Power law first order

Time (min)	Ln(C)							
	Exp 1	Exp 2	Exp 3	Exp 4	Exp 5	Exp 6	Exp 7	Exp 8
30	8.118	7.513	8.976	8.271	8.755	8.670	8.950	7.343
60	8.707	7.947	9.194	8.627	8.951	8.868	9.140	9.617
90	8.918	7.977		8.725	9.167	9.093	9.412	9.785
120	9.032	8.097	9.585	8.908	9.429	9.277	9.738	9.805
180	9.199	8.238	9.644	9.040		9.474		10.080
240	9.226	8.284	9.622	9.169	9.960	9.758	10.489	10.311
360	9.308	8.540	9.778	9.415	10.197	10.033	10.865	10.655

Power law second order

Time (min)	1/C							
	Exp 1	Exp 2	Exp 3	Exp 4	Exp 5	Exp 6	Exp 7	Exp 8
30	2.98E-04	5.46E-04	1.26E-04	2.56E-04	1.58E-04	1.72E-04	1.30E-04	6.47E-04
60	1.65E-04	3.54E-04	1.02E-04	1.79E-04	1.30E-04	1.41E-04	1.07E-04	6.66E-05
90	1.34E-04	3.43E-04		1.62E-04	1.04E-04	1.12E-04	8.17E-05	5.63E-05
120	1.19E-04	3.05E-04	6.88E-05	1.35E-04	8.03E-05	9.35E-05	5.90E-05	5.52E-05
180	1.01E-04	2.64E-04	6.48E-05	1.19E-04		7.68E-05		4.19E-05
240	9.85E-05	2.53E-04	6.62E-05	1.04E-04	4.73E-05	5.78E-05	2.79E-05	3.33E-05
360	9.07E-05	1.95E-04	5.67E-05	8.15E-05	3.73E-05	4.39E-05	1.91E-05	2.36E-05

Power law third order

Time (min)	$1/2C^2$							
	Exp 1	Exp 2	Exp 3	Exp 4	Exp 5	Exp 6	Exp 7	Exp 8
30	4.45E-08	1.49E-07	7.99E-09	3.27E-08	1.24E-08	1.47E-08	8.42E-09	2.09E-07
60	1.37E-08	6.26E-08	5.16E-09	1.61E-08	8.39E-09	9.93E-09	5.76E-09	2.21E-09
90	8.98E-09	5.89E-08		1.32E-08	5.45E-09	6.33E-09	3.34E-09	1.58E-09
120	7.14E-09	4.64E-08	2.36E-09	9.15E-09	3.23E-09	4.37E-09	1.74E-09	1.52E-09
180	5.11E-09	3.50E-08	2.10E-09	7.03E-09		2.95E-09		8.79E-10
240	4.85E-09	3.19E-08	2.19E-09	5.43E-09	1.12E-09	1.67E-09	3.88E-10	5.53E-10
360	4.12E-09	1.91E-08	1.61E-09	3.32E-09	6.95E-10	9.64E-10	1.83E-10	2.78E-10

Empirical model 1

Time (min)	$X_{Predicted}$							
	Exp 1	Exp 2	Exp 3	Exp 4	Exp 5	Exp 6	Exp 7	Exp 8
30	0.106	0.058	0.125	0.062	0.201	0.034	0.015	0.001
60	0.137	0.068	0.142	0.076	0.293	0.051	0.022	0.057
90	0.167	0.077	0.159	0.089	0.372	0.079	0.038	0.079
120	0.195	0.087	0.175	0.103	0.442	0.115	0.072	0.082
180	0.249	0.106	0.206	0.129	0.562	0.170		0.143
240	0.299	0.124	0.236	0.154	0.653	0.300	0.323	0.226
360	0.391	0.160	0.293	0.203	0.794	0.520	0.686	0.450

Empirical model 2

Time (min)	$X_{Predicted}$							
	Exp 1	Exp 2	Exp 3	Exp 4	Exp 5	Exp 6	Exp 7	Exp 8
30	0.106	0.058	0.125	0.062	0.201	0.184	0.122	0.024
60	0.135	0.068	0.142	0.075	0.277	0.237	0.235	0.100
90	0.163	0.077	0.158	0.089	0.346	0.287	0.334	0.171
120	0.191	0.087	0.173	0.102	0.410	0.334	0.423	0.236
180	0.244	0.105	0.204	0.128	0.527	0.422	0.580	0.358
240	0.294	0.124	0.234	0.154	0.625	0.501	0.701	0.463
360	0.388	0.160	0.292	0.203	0.788	0.640	0.888	0.644

Empirical model 3

Time (min)	$X_{Predicted}$							
	Exp 1	Exp 2	Exp 3	Exp 4	Exp 5	Exp 6	Exp 7	Exp 8
30	0.106	0.058	0.125	0.062	0.201	0.184	0.122	0.024
60	0.169	0.075	0.150	0.085	0.353	0.277	0.319	0.276
90	0.206	0.088	0.171	0.101	0.426	0.333	0.380	0.293
120	0.235	0.099	0.188	0.114	0.480	0.376	0.427	0.309
180	0.285	0.118	0.219	0.138	0.570	0.449	0.506	0.338
240	0.323	0.133	0.245	0.156	0.636	0.504	0.566	0.364
360	0.388	0.160	0.290	0.189	0.740	0.594	0.662	0.411

Empirical model 4

Time (min)	(1 - X) + XlnX							
	Exp 1	Exp 2	Exp 3	Exp 4	Exp 5	Exp 6	Exp 7	Exp 8
30	0.656	0.777	0.615	0.766	0.040	0.034	0.015	0.001
60	0.492	0.695	0.555	0.697	0.060	0.051	0.022	0.057
90	0.423	0.688		0.676	0.092	0.079	0.038	0.079
120	0.383	0.661	0.432	0.632	0.155	0.115	0.072	0.082
180	0.323	0.626	0.411	0.598		0.170		0.143
240	0.314	0.614	0.419	0.562	0.449	0.300	0.323	0.226
360	0.284	0.543	0.365	0.487	0.721	0.520	0.686	0.450

Appendix C

Summary of R^2 values for K model fits (Hydrochloric acid)

Exp	Empirical 1	Empirical 2	Empirical 3	Empirical 4	Shrinking core reaction rate (Sphere)	Shrinking core external mass (Sphere)	Shrinking core ash (Plate)	Shrinking core ash (Sphere)	first order	2nd order	3rd order
1	0.916	0.921	0.844	0.957	0.954	0.954	0.944	0.941	0.957	0.948	0.926
2	0.227	0.234	0.125	0.572	0.58	0.58	0.586	0.587	0.567	0.551	0.532
3	0.796	0.804	0.682	0.914	0.869	0.871	0.812	0.8	0.929	0.948	0.931
4	0.988	0.99	0.92	0.996	0.993	0.994	0.966	0.96	0.988	0.944	0.872
5	0.98	0.98	0.849	0.813	0.972	0.964	0.974	0.984	0.841	0.709	0.575
6	0.824	0.796	0.809	0.669	0.742	0.74	0.753	0.749	0.621	0.448	0.324
7	0.943	0.959	0.099	0.923	0.985	0.985	0.962	0.951	0.875	0.627	0.429
8	0.843	0.811	0.942	0.623	0.796	0.785	0.846	0.874	0.615	0.471	0.355
Average	0.815	0.812	0.659	0.808	0.861	0.859	0.855	0.856	0.799	0.706	0.618
Std dev	0.2480518	0.2472	0.3465	0.1653	0.147	0.1472	0.1366	0.1367	0.1709	0.2157	0.2558

Summary of R^2 values for overall model fits (Hydrochloric acid)

Exp	Empirical 1	Empirical 2	Empirical 3	Empirical 4	Shrinking core reaction rate (Sphere)	Shrinking core external mass (Sphere)	Shrinking core ash (Plate)	Shrinking core ash (Sphere)	first order	2nd order	3rd order
1	0.828	0.971	0.912	0.971	0.976	0.977	0.967	0.963	0.968	0.937	0.885
2	0.921	0.044	0.908	0.954	0.944	0.944	0.906	0.901	0.950	0.909	0.833
3	0.874	0.948	0.945	0.944	0.950	0.951	0.931	0.924	0.927	0.862	0.771
4	0.967	0.998	0.919	0.984	0.998	0.998	0.975	0.968	0.957	0.848	0.710
5	0.968	0.973	0.825	0.771	0.952	0.942	0.953	0.970	0.799	0.644	0.494
6	0.988	0.795	0.904	0.649	0.741	0.737	0.759	0.765	0.646	0.541	0.438
7	0.901	0.975	0.482	0.903	0.983	0.981	0.974	0.967	0.870	0.666	0.480
8	0.913	0.766	0.884	0.591	0.757	0.746	0.784	0.817	0.614	0.511	0.416
Average	0.920	0.809	0.847	0.846	0.913	0.909	0.906	0.909	0.841	0.740	0.629
Std dev	0.054	0.322	0.152	0.155	0.103	0.106	0.086	0.078	0.142	0.169	0.191

Summary of R^2 values for K model fits (Nitric acid)

Exp	Empirical 1	Empirical 2	Empirical 3	Empirical 4	Shrinking core reaction rate (Sphere)	Shrinking core external mass (Sphere)	Shrinking core ash (Plate)	Shrinking core ash (Sphere)	first order	2nd order	3rd order
1	0.723	0.703	0.786	0.558	0.781	0.765	0.819	0.864	0.594	0.48	0.386
2	0.705	0.695	0.77	0.637	0.731	0.725	0.784	0.804	0.623	0.539	0.461
3	0.739	0.716	0.783	0.583	0.695	0.686	0.701	0.73	0.61	0.559	0.509
4	0.874	0.863	0.945	0.787	0.899	0.893	0.949	0.964	0.765	0.641	0.526
5	0.893	0.95	0.857	0.839	0.947	0.983	0.966	0.951	0.922	0.881	0.83
6	0.955	0.961	0.916	0.793	0.969	0.961	0.963	0.979	0.859	0.771	0.676
7	0.693	0.817	0.513	0.803	0.925	0.956	0.984	0.916	0.932	0.866	0.785
8	0.878	0.846	0.943	0.511	0.892	0.872	0.958	0.978	0.468	0.251	0.185
Average	0.807	0.819	0.814	0.689	0.855	0.855	0.891	0.898	0.722	0.623	0.545
Std dev	0.10275352	0.1065	0.1416	0.1302	0.1043	0.1153	0.1069	0.0915	0.1724	0.2131	0.2137

Summary of R^2 values for K model fits (Nitric acid)

Exp	Empirical 1	Empirical 2	Empirical 3	Empirical 4	Shrinking core reaction rate (Sphere)	Shrinking core external mass (Sphere)	Shrinking core ash (Plate)	Shrinking core ash (Sphere)	first order	2nd order	3rd order
1	0.7231	0.7032	0.7863	0.7308	0.8713	0.8645	0.9388	0.9494	0.6746	0.4918	0.3543
2	0.7048	0.6952	0.7703	0.9144	0.9556	0.9543	0.9850	0.9855	0.8500	0.6938	0.5312
3	0.7389	0.7163	0.7830	0.8180	0.8869	0.8836	0.9306	0.9370	0.7856	0.6871	0.5951
4	0.8738	0.8631	0.9447	0.9481	0.9810	0.9801	0.9916	0.9899	0.8959	0.7606	0.6136
5	0.8928	0.9504	0.8572	0.8528	0.9804	0.9962	0.9722	0.9664	0.8925	0.7882	0.6611
6	0.9549	0.9612	0.9160	0.8454	0.9829	0.9777	0.9860	0.9856	0.8635	0.7244	0.5828
7	0.6926	0.8167	0.5134	0.8984	0.9754	0.9710	0.9790	0.9137	0.9305	0.7953	0.6397
8	0.8776	0.8455	0.9431	0.5940	0.9471	0.9338	0.9923	0.9873	0.4529	0.2112	0.1702
Average	0.8073	0.8190	0.8143	0.8252	0.9476	0.9451	0.9719	0.9643	0.7932	0.6441	0.5185
Std dev	0.102742	0.106518	0.14143	0.11466	0.044355407	0.047901234	0.023956	0.02832	0.15919	0.199507	0.1700762